Earth-Science Reviews 257 (2024) 104902

Contents lists available at ScienceDirect

Earth-Science Reviews

journal homepage: www.elsevier.com/locate/earscirev

Insights into the role of tectonic extension and compression vs. subduction erosion in the tectonics of forearcs: Examples from the Japan Trench and the Middle America Trench

Paola Vannucchi[a,*], Jason P. Morgan[b]

[a] Earth Science Department, University of Florence, Italy
[b] ICM-CSIC, Barcelona, Spain

ARTICLE INFO

Keywords:
Subduction erosion
Forearc extension
Forearc compression
Japan Trench
Middle America Trench

ABSTRACT

The forearc region remains key in understanding the dynamics of convergent plate tectonics. This study focuses on the mechanisms governing tectonic processes within the overriding plate forearc which spans from the trench to the volcanic arc at two key and relatively well studied regions: the Japan Trench and the Middle America Trench offshore SE Costa Rica. We address the questions that have arisen concerning material input into the plate boundary, whether by subduction, accretionary prism formation, or tectonic erosion. In the Japan Trench case study, while tectonic accretion occurs near the trench axis, significant forearc subsidence suggests net material removal, possibly through tectonic erosion that has transferred material to the subducting slab. Debate surrounds the mechanism driving forearc subsidence, with recent studies proposing extensional tectonism as a possible mechanism to exclude subduction erosion. However, seismic evidence challenges this hypothesis, as normal faults indicative of forearc extension are not prominent. Moreover, a quantitative mass-balance analysis fails for the forearc if extensional tectonics rather than tectonic erosion is assumed to have predominantly shaped the margin. The spatio-temporal progression of subsidence across the forearc is further explored; this indicates that peak subduction erosion has occurred beneath the lower slope. The Middle America Trench in SE Costa Rica has also been extensively studied with several drilling expeditions, with particular focus on the area where the aseismic Cocos Ridge is subducting beneath the Caribbean plate. Here the subduction of topographic relief has been traditionally viewed as a process that enhances subduction erosion. Recent studies have challenged this perspective, suggesting instead that subducting topography might lead to net accretion to the margin through various mechanisms. Ocean drilling expeditions provide valuable data on sedimentary successions and forearc tectonic evolution. These drilling data have been not always used to the best of their capacity, which has led to significant discrepancies between drilling-based inferences and seismic interpretations, in particular regarding the presence and nature of unconformities within the forearc sediments. Borehole observations strongly favor the inference that inboard the Cocos Ridge a large amount of subsidence has occurred, linked to recent subduction erosion beneath this forearc.

Table of Acronyms

CRISP	Costa Rica Seismogenesis Project
DSDP	Deep Sea Drilling Project
ODP	Ocean Drilling Program
IODP	Integrated Ocean Drilling Program
IPOD	International Phase of Ocean Drilling
RBU	Regional Basal Unconformity (Japan)
PFZ	Panama Fracture Zone
PTJ	Panama Triple Junction

1. Introduction

Convergent plate margins are where most of Earth's global seismic energy is released (Bilek and Lay, 2018). Subduction zones link Earth's surface processes with its interior, and so shape many geochemical cycles, including water (Rupke et al., 2004) and carbon (Plank and Manning, 2019). However, ever since broad acceptance of the concept of

* Corresponding author.
E-mail address: paola.vannucchi@unifi.it (P. Vannucchi).

https://doi.org/10.1016/j.earscirev.2024.104902
Received 14 June 2024; Received in revised form 14 August 2024; Accepted 15 August 2024
Available online 16 August 2024

subducting lithosphere (Isacks et al., 1968), the scientific community has engaged in a debate regarding the tectonic processes that occur within the subducting plate's overriding forearc. This tectonic region extends from the trench to the volcanic arc. It can strongly shape material input into the plate boundary (Karig and Sharman, 1975; von Huene and Lallemand, 1990). Debate still focusses on a first order problem concerning the transfer of material between the subducting and overriding plates: does subduction convey most trench sediments into the plate boundary, or only a fraction of them leaving the rest able to pile-up in front of the overriding plate to build an accretionary prism? Or instead, can subduction even induce net removal of material from the overriding plate through tectonic erosion? While evidence indicating the underthrusting and accretion of sediments was early and widely accepted, evidence indicating tectonic erosion of forearc material has always been more elusive since it is in the form of clues that imply missing material instead of added material. Unlike underthrusted and accreted material which can be imaged and seen in the geologic record of fossil subduction zones, subduction erosion removes material that can only be traced geochemically, by its effects on the melting which generates a volcanic arc (Straub et al., 2020). The use of 2D and 3D reflection seismics, for example, cannot image missing material. Even imaging of an ongoing erosive process might not be interpreted as evidence that removal is occurring, since seismic interpretations often need to rely on assumptions, for example that only erosive margins possess subduction channels, or that erosion is possible only where the incoming plate is characterized by horst-and-graben structures (Edwards et al., 2021). One of the most widely used proxies to infer and then quantify the magnitude of subduction erosion is measurements of forearc subsidence. This has recently led to a search for alternative models to explain forearc subsidence, models that in turn will affect current estimates of subduction zone mass balances through their assumptions of net extension or compression in various forearcs. In the last decade, for example, changes in forearc mass have sometimes been attributed to changes in plate kinematics that drive the onset of extensional tectonics within the forearc (Regalla et al., 2013), or alternatively to forearc-arc-backarc shortening that drives compressional tectonics within the forearc (Morell et al., 2019). Here we will reassess whether forearc extension or compression are indeed viable conceptual scenarios to forearc subduction erosion as done in these recent estimates of mass balances in the conventionally-viewed "erosive" margins of NE Japan and SW Costa Rica.

2. Japan Trench

In 1977, the Japan Trench was drilled to test the accretionary prism model (Arthur and Adelseck, 1980) as part of the Deep Sea Drilling Program (DSDP), Legs 56–57, within the International Phase of Ocean Drilling (IPOD) (Fig. 1). The general plan was to drill along a transect from the incoming plate near the trench to the forearc. The recovered sediments were anticipated to show that the forearc would have progressively older ages when going from the outer to the inner forearc, and that the forearc slope/apron would show evidence of progressive uplift consistent with landward thickening of the forearc wedge.

2.1. Ocean drilling data

To the surprise of the IODP scientists, ongoing regional subsidence — not uplift — was unexpectedly recognized at Site 439 located on the

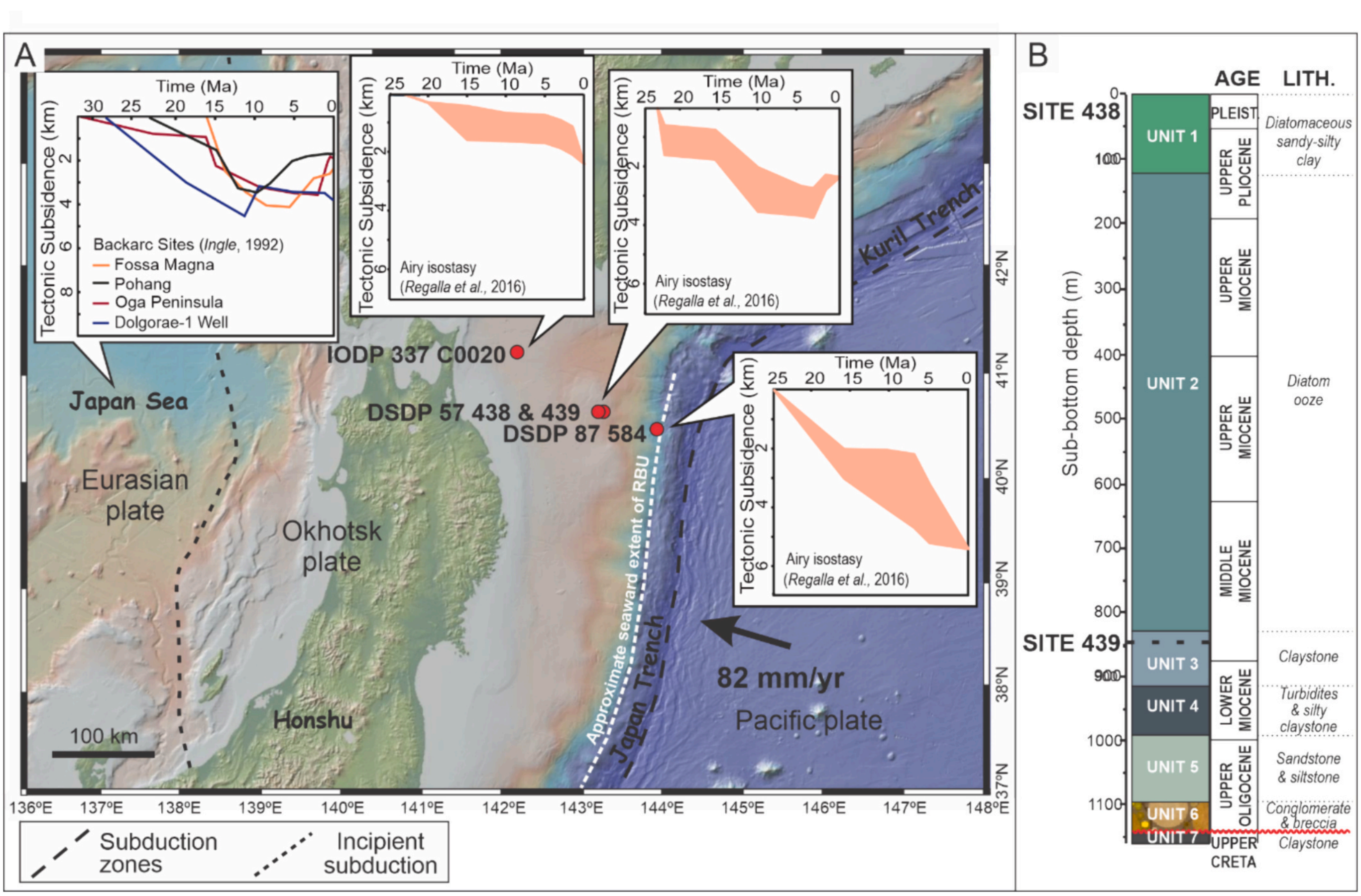

Fig. 1. (A) Bathymetry, topography (http://www.geomapapp.org, Ryan et al., 2009), and the tectonic plate configuration in the Japan Trench region. Arrows show plate motions with respect to the Eurasian plate (DeMets et al., 1990). Insets show the published tectonic subsidence curves for sites in the Sea of Japan (Ingle, 1992), and Japan Trench forearc (Regalla et al., 2013). B) Reconstructed sedimentary column from DSDP Sites 438 and 439.

lower slope (40.6268, 143.3105) ≈ 100 km landward from the trench axis (Fig. 1). There, in 1560 m water depth and ≈1200 m below sea floor (mbsf), the base of the slope sediments consists of Oligocene non-marine conglomerates with dacitic boulders that rest unconformably on top of tilted Upper Cretaceous siltstones deposited in a deep water (>2000 m) environment. These Mesozoic sediments below the angular unconformity could have either been accreted to the margin before the Oligocene, or formed part of a Cretaceous forearc sequence. Unfortunately no conclusive data were found by drill sampling, even though the shipboard party slightly preferred the interpretation of an accreted sequence (von Huene et al., 1982). The conglomerates above the unconformity are 48 m thick, unconsolidated, and with horizontal bedding. They are covered by ≈ 50 m of lower Miocene sandstones with abundant and little transported macrofossils (von Huene et al., 1978). These drillcore data established that, between the late Cretaceous (at the earliest) and the Oligocene, the area drilled at Site 439 was uplifted from a deep-water environment to subaerial conditions. The above complete lower Miocene to Pleistocene slope sediment section recovered at Site 439 and adjacent Site 438 (40.6298, 143.2358) also independently provided data to show that ever since ≈ 22 Ma ago the upper slope has been characterized by subsidence (Arthur et al., 1980; Keller, 1980) (Fig. 1) with minimum average subsidence rates of ~140 m/my (von Huene and Lallemand, 1990). Further investigations were carried out during DSDP Leg 87 at Site 584. This site was designed to again drill and core the unconformity. It only reached middle Miocene sediments at 950 mbsf, with data confirming lower bathyal-abyssal paleo-depths in the Pliocene (Kagami et al., 1986) (Fig. 1).

Seismic reflection studies indicate that the reflector correlated with the Oligocene subaerial erosive unconformity that was drilled during Leg 57 has a regional extent (Nasu et al., 1980; von Huene et al., 1982; Tsuru et al., 2000; Tsuru et al., 2002; Boston et al., 2017). This reflector, called the Regional Basal Unconformity – RBU – characterizes the Japan Margin from its upper to lower forearc slope, reaching 10 km from the trench axis in some areas. It extends laterally for hundreds of kilometers (Fig. 1).

3. Discussion

This combination of geophysical data and drill sampling-based results indicates that tectonic accretion is presently occurring here in only a small frontal zone that extends from a few km to a maximum of ≈30 km from the trench axis (Arthur and Adelseck, 1980; von Huene et al., 1982; Tsuru et al., 2000). This potentially accreted volume is much too small to accommodate all sediments transported by the subducting plate into the trench during the Neogene. Moreover, the observed massive subsidence of the leading edge of the Japanese forearc implies a net subtraction of mass from the forearc margin. This was proposed to occur through the process of tectonic erosion, whereby material is removed from the base of the upper plate (von Huene and Culotta, 1989; von Huene and Lallemand, 1990) and transferred to the downgoing subducting slab. Estimates of local mass removal from the upper plate range between 55 and 84 km^3/Myr per km of trench along strike (von Huene and Lallemand, 1990; Straub et al., 2020).

Since the drilling observations obtained in DSDP Leg 87, the occurrence of Neogene subsidence in the Japan Trench margin has not been argued, although the potential mechanism(s?) leading to this subsidence have been periodically revisited. In particular extensional tectonism in the forearc has been repeatedly proposed as an alternative process that could lead to forearc subsidence (Karig et al., 1983). Recently forearc extension has been reconsidered by Regalla et al. (2013), who noted that subsidence occurred at the same time as the opening of the Japan Sea. They inferred from this temporal coincidence that the same mechanism – extension – was responsible for both Japan Sea opening and the Japan Trench's forearc subsidence (Fig. 1). Regalla et al. (2013) proposed there was a uniform factor of 2 extension of the entire forearc-arc-backarc system. However, while in the Japan Sea the crustal thinning related to local subsidence is well imaged seismically (Sato, 1994), the Japan forearc lacks any evidence of extensive normal faulting (Boston et al., 2017; Park et al., 2021). While normal faults in the Japan Trench forearc contribute to the deformation and subsidence of the forearc slope, they do not account for a significant amount of large scale stretching (Boston et al., 2017). This presents the first difficulty in accepting this proposed thinning mechanism. In addition, the seismic line located near the nucleation area of the 2011 Tohoku earthquake, approximately 200 km south of Sites 438/439, indicates that the normal faults there show little normal displacement, further supporting their limited role in causing significant stretching. Therefore, while normal faults can influence local tectonic processes and morphological changes, other mechanisms are needed to explain the significant thinning of the forearc.

A second quantitative problem arises when we consider that the assumed absence of subduction erosion would imply that the original volume of the forearc has been preserved as it extended to its present configuration. In this case the forearc volume trenchward of Site 439 should correspond to the volume of the Oligocene forearc from the paleo-coast – well-marked by the subaerial erosion unconformity - to the trench. The modern forearc has a thickness of ≈50 km beneath the coastal area currently located ≈200 km from the trench (Hayes et al., 2018) while its crustal thickness beneath the coast is ≈28 km (Takahashi et al., 2004; Wang and Zhao, 2005; Iwasaki et al., 2013). This would imply an upper plate cross-sectional volume of ≈3200 km^2 per km of trench along strike (Fig. 2). The forearc beneath the Oligocene coastline Site 439 is ≈15 km thick (von Huene and Culotta, 1989; von Huene and Lallemand, 1990; Tsuru et al., 2000; Takahashi et al., 2004) which would imply that the current cross-sectional volume of forearc seaward of Site 439 is 750 km^2 per km of trench — a factor of 4 too small (Fig. 2). The crustal thickness value calculated at Site 439 is also in agreement with the crustal thickness in the case where a factor of 2 for extension is applied to the crust of the forearc as proposed by Regalla et al. (2013). From this calculation it is easy to infer that, compared to the modern forearc profile, there is a volume deficit of ≈2500 km^2 (3200–750 = 2450) per km of trench. Assuming the forearc extension scenario, we can assume that the maximum pre-extension volume of the Japan submarine forearc was ≈750 km^2 per km of trench (Fig. 2).

From this we can try to reconstruct the Oligocene forearc profile and critical taper angle – even though we know that most of today's forearc volume seaward of Site 439 is due to a modern frontal prism that was quite possibly not even present during the Oligocene. To maintain a forearc thickness of 50 km the coast should have been located at ≈30 km from the trench. Simple trigonometry would imply an unrealistic taper angle of ≈80°. Even if we limit the maximum forearc thickness to 28 km – the present-day coastline crustal thickness – the current calculated cross-sectional volume is ≈2800 km^2 per km of trench which leads to an Oligocene volume deficit of ≈2000 km^2 per km of trench. In this case to maintain a crustal thickness of 28 km the coast should have been located at ≈53 km from the trench which would imply a taper angle of ≈27°, which is ≈60% higher than the highest taper angles measured in today's global trench systems, i.e. at the Philippine Trench and South Sandwich Trough (Clift and Vannucchi, 2004).

Although unrealistic to maintain this state, the critical wedge theory for an accretionary prism would need either excessively high or low values of parameters such as basal and internal friction and fluid pressure (Davis et al., 1983). Interestingly the inferred taper angles would also fall in the ranges of supercritically tapered wedges that characterize forearcs with no accretion that are instead undergoing active tectonic erosion (Davis et al., 1983). Furthermore, from the mass balance calculation, it is evident that extension would also not explain why the Oligocene mantle forearc is now missing (Fig. 2).

These simple mass-balance calculations show that while extension is obviously conceivable as a potential subsidence mechanism, the observed crustal thinning in the forearc strongly implies the involvement of net removal of forearc material. The synchronicity of

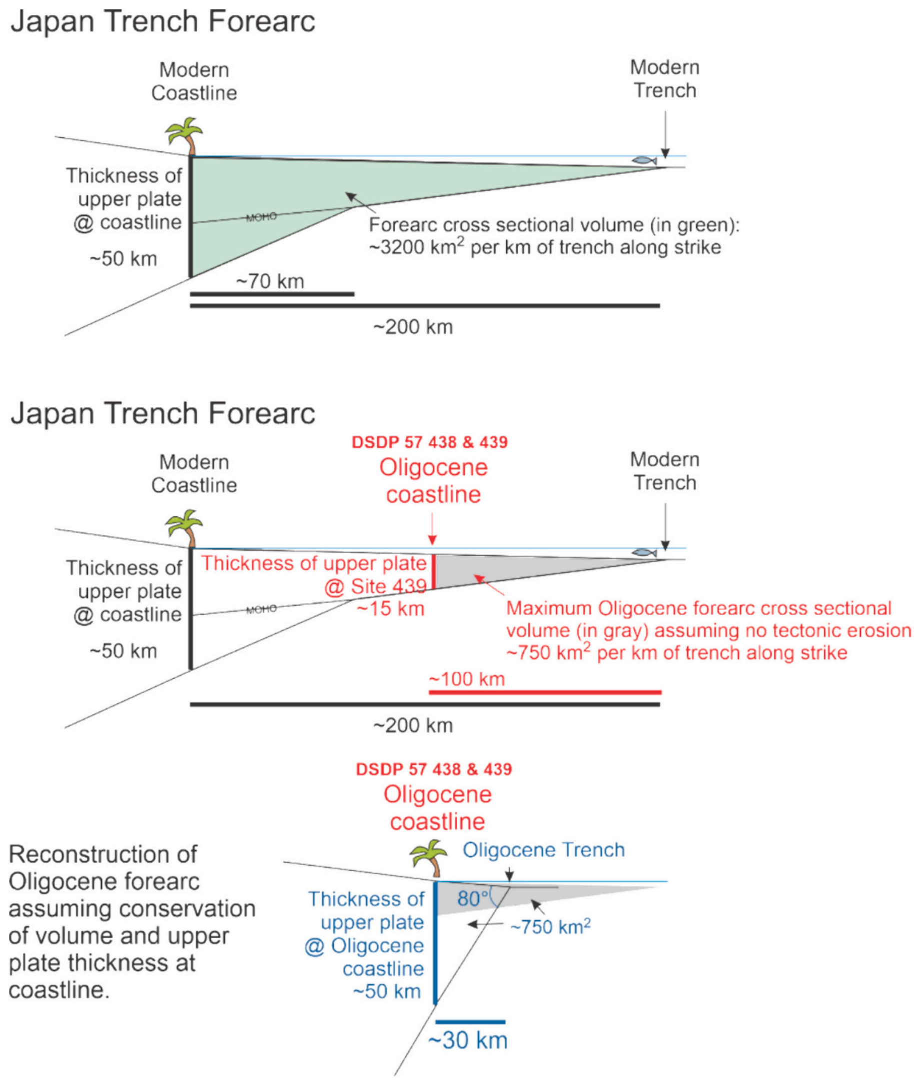

Fig. 2. Geometric reconstruction of the forearc geometry in the Oligocene – age of the subaerial unconformity recovered at DSDP Site 439 – assuming conservation of volume – non erosive margin – and with an upper plate geometry similar to the present one (Iwasaki et al., 2013; Hayes et al., 2018).

deformation events in the upper plate linked both to the opening of the Japan Sea and subduction erosion is interesting, and should be considered, but in scenarios in which there is a potential causal link between them, instead of the hypothesis that Japan Sea subsidence and Japan forearc subsidence were directly caused by the same extensional process. For example, a possible shallowing of the Pacific paleoslab dip could have been a byproduct of the opening of the Japan Sea, that in turn caused the forearc to migrate over the subducting plate which either triggered or enhanced subduction erosion.

The subsidence curve of Sites 438/439 is characterized by an initial phase between ≈25 and ≈15 Ma with low subsidence rates of 0.05–0.1 km/Ma, followed by a second phase between ≈15 and ≈5 Ma of faster subsidence rates of 0.1–0.2 km/Ma (Arthur et al., 1980; Regalla et al., 2013) (Fig. 1). It is interesting to note that the subsidence curve reconstructed from a drilled site located on the shelf (41.176638; 142.200547) - ≈ 50 km from the Honshu Island coast – is characterized by subsidence with rates similar to the slow phase at Sites 438/439. At DSDP Site 584 (40.4667; 143.9517), located at ≈50 km from the trench, the rates are similar to the fast phase of Sites 438/439. This trend is further confirmed by the RBU geometry which shows a uniform increase in depth towards the east, i.e. towards the trench axis (Boston et al., 2017). In the absence of direct drilling data, forearc sediment thickness can account for subsidence, if not affected by mass-wasting deposits. So, the fact that the RBU increases in depth towards the east would imply progressively higher subsidence towards the trench. This spatio-temporal progression of subsidence across the shelf and slope also characterizes other erosive margins, such as the Guatemala Trench (Vannucchi et al., 2004). This progression suggests that peak subduction erosion occurs under the lower slope of the forearc where the upper plate crust lies directly on top of the subducting slab without intervening mantle lithosphere between the two, therefore not involving the erosion of forearc lithospheric mantle. Even if tectonic erosion of forearc lithospheric mantle were to occur (Lallemand et al., 1992; Regalla et al., 2013; Lallemand et al., 2024), the lower-than normal-density of the eroded mantle wedge material would be isostatically ‘replaced’ with an equal thickness of higher density mantle that underlies the subducting crust- which would not induce isostatic uplift. It is worth noting that because the subducting ocean crustal layer maintains a constant thickness in these isostatic calculations, its isostatic effects can be ignored.

Another outcome of peak subduction erosion occurring beneath the forearc slope is that this would also be the region where the largest subducted sediment dehydration would be anticipated to occur (Ranero et al., 2008), which provides the potential for large fluid volumes to be released that would raise pore pressure and favor upward migration of the plate boundary (von Huene et al., 2004). In this regard, irrespective of a subduction margin being accretionary, non-accretionary or erosive, the plate boundary beneath the forearc slope is anticipated to be characterized by high fluid pressure (Saffer and Tobin, 2011). This in turn could influence the permanent deformation characteristics of the forearc, with normal faults potentially forming when the upper plate and the overriding plate are poorly coupled – as to be expected in a region of high pore pressure (Wang and Hu, 2006; Wang et al., 2010) – and folds and reverse faults forming when the plates are more strongly coupled. The dehydration peak being confined to a specific region, the spatiotemporal progression of subduction erosion, and dynamic stress fluctuations linked to the earthquake cycle, could all lead to complex deformation patterns that include not only normal faults, but also compressional structures.

In summary, while at the Japan Trench forearc subsidence has long been proposed to have been due to extensional tectonism (Karig et al., 1983), more recent geophysical studies do not show evidence of major extensional normal faults that cut the forearc (Boston et al., 2017; Park et al., 2021). Furthermore, extensional tectonism does not provide a quantitative mechanism to generate the observed present-day forearc volume, while paleo-forearc reconstructions are also not in accord with either the critical Coulomb wedge theory or the observed geometries of modern forearcs. Finally, models that envision extensional tectonism as being the principal driver for forearc subsidence still actually require later subduction erosion to achieve the observed subsidence (Regalla et al., 2013).

4. Middle America Trench – SE Costa Rica Subduction system

The Middle America Trench has been the subject of four drilling transects: DSDP Leg 66 offshore Mexico (Watkins and Moore, 1981), DSDP Legs 67 and 84 offshore Guatemala (Aubouin and von Huene, 1982; von Huene and Aubouin, 1984), ODP Legs 84, 170 and 205 offshore Northern Costa Rica (von Huene and Aubouin, 1984; Kimura et al., 1997; Morris et al., 2003), and IODP Exp. 334 and 344 offshore southern Costa Rica (Vannucchi et al., 2012; Harris et al., 2013) (Fig. 3).

Our attention is directed towards the southern Costa Rica transect drilled during IODP Exp. 334 and 344, a distinct area where the aseismic Cocos Ridge currently subducts beneath the Caribbean plate (Fig. 3). This geological setting represents approximately 10% of the overall 3000-km length of the Middle America Trench (Fig. 3). It is important to note that, unlike the Japan Trench where the primary argument against subduction erosion centers on margin extension, in southern Costa Rica the argument against subduction erosion has been tied to margin contraction, specifically contraction driven by forearc-arc-backarc shortening processes (Morell et al., 2019), that are deemed to not result in significant forearc loss (Edwards et al., 2021).

The Cocos Ridge is a 200 km-wide aseismic ridge. The Cocos Ridge crust has an estimated average thickness of 16.5–19 km, while the Cocos plate crust away from the ridge is ≈ 7–10 km thick (Sallares et al., 2003). It is responsible for topographic relief that can reach 2000 m above normal depths for ~20 Ma seafloor. To its SE the subducting Cocos Ridge is bordered by the Panama Fracture Zone (PFZ). The PFZ separates the Cocos plate to the W, which is subducting at ≈ 90 mm/yr and almost perpendicular beneath the Caribbean plate, from the Nazca plate to the E, which is obliquely subducting at ≈40 mm/yr under the South American plate (Fig. 3). The intersection of the PFZ with the Central America Trench represents the Panama Triple junction between the Cocos, Nazca and Caribbean plates. The Panama Triple Junction has been migrating to the southeast at a rate of ≈ 30–55 mm/yr (McIntosh et al., 1993; Kobayashi et al., 2014; Morell, 2015; Morell, 2016).

Further to the east the Balboa and Coiba fracture zones are located at

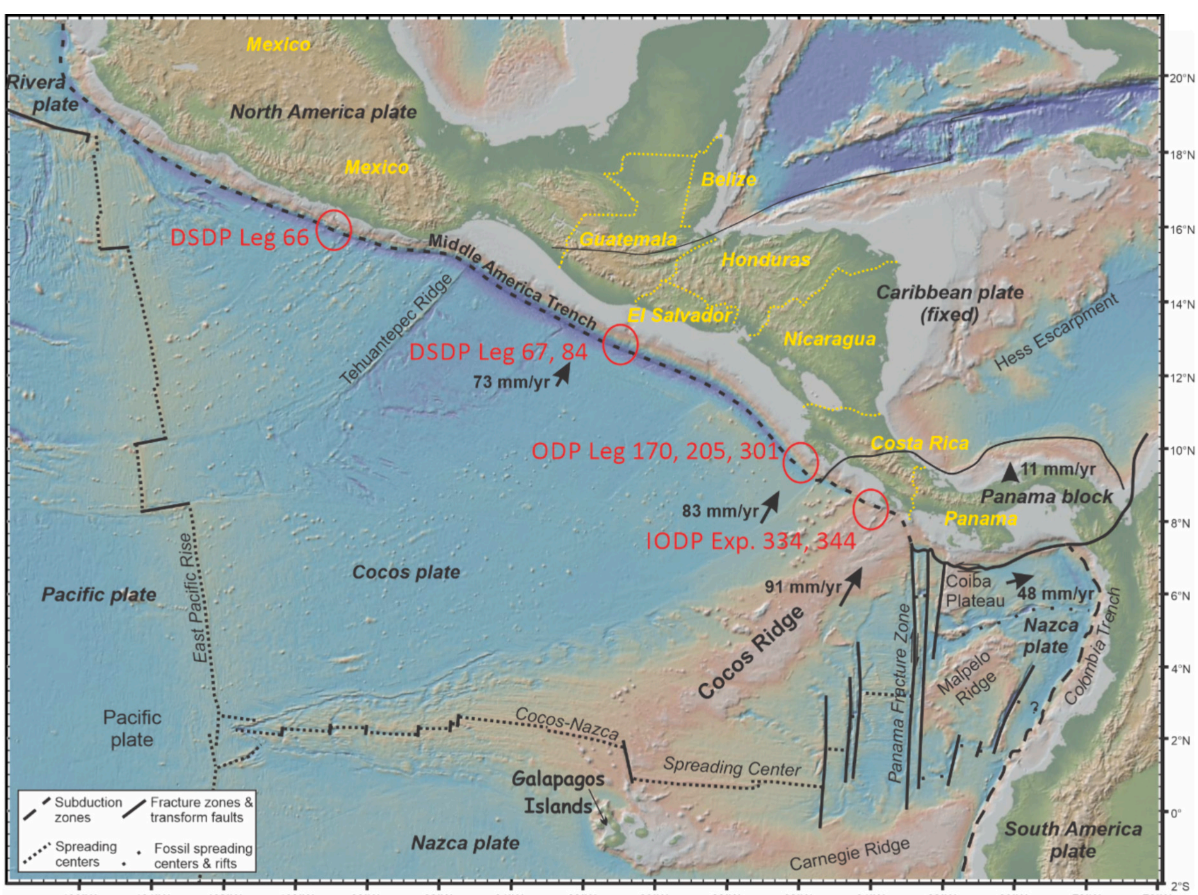

Fig. 3. Bathymetry, topography (http://www.geomapapp.org, Ryan et al., 2009), and the tectonic plate configuration along the Middle America Trench with location of the DSDP, ODP and IODP drilling expeditions. Arrows show plate motions with respect to the Caribbean plate (DeMets et al., 1990; DeMets, 2001).

≈50 and ≈100 km from the PFZ, respectively (Fig. 3). These three fracture zones seem to be related to the Cocos-Nazca plate boundary, with the Coiba fracture zone possibly being the plate boundary prior to ≈ 2 Ma (MacMillan et al., 2004). To the east of the Coiba fracture zone, the Coiba ridge is a ≈ 2000 m-high bathymetric feature covering an area of ≈100kmx150km and with a steep slope to the west and a gentle slope to the east (Fig. 3). The nature of the Coiba ridge seems to be related to compression-driven uplift adjacent to the migrating triple junction (MacMillan et al., 2004). Dynamic uplift in the forward corner of the migrating triple junction might have been present also in the past. A different origin is inferred for the Malpelo ridge, situated still to the east of the Coiba fracture zone, but further to the south (Fig. 3). The Malpelo ridge is interpreted to be an offset portion of the Cocos Ridge (Hoernle et al., 2002). Interestingly no fragments of the hotspot track are present within the fracture zone system.

To the NW of the Cocos Ridge the subducting Cocos Plate is punctuated by seamounts (Fig. 4). The subducting seamounts are responsible for indentations in the trace of the frontal thrust and breaches in the Costa Rica forearc slope, damage that has been quickly restored by secondary processes such as mass wasting (von Huene et al., 2000). In general subducting seamounts cause both transient tectonic activity (Husen et al., 2002; Bilek et al., 2003) and vertical movements across a corridor that involves the entire forearc (Fisher et al., 1998; Gardner et al., 2001).

Subduction of topographic relief has long been recognized to be a mechanism that can cause localized subduction erosion, mostly by abrasion of the overriding plate (Hilde, 1983; von Huene et al., 2004; Bangs et al., 2006). Similar to the subduction of seamounts, the subduction of aseismic ridges is typically seen as a process that enhances subduction erosion (Bangs and Cande, 1997; Clift and MacLeod, 1999; Clift et al., 2003; Stern, 2011). However lately its effects have been reconsidered to the point that some authors consider subducting topography provides an alternative mechanism to subduction erosion (Edwards et al., 2018; Morell et al., 2019; Edwards et al., 2021) and is a potential cause for net accretion to the margin (Bangs et al., 2016).

In fact, although it is recognized that subducting topography can cause material removal from the frontal prism and lower slope, these authors posit that at depth it could induce net upper plate thickening that drives subsidence by flexural loading and forearc shortening while delivering a thick sediment pile to the trench. This is particularly controversial in the case of the subduction of the Cocos Ridge (Morell et al., 2019). The most notable effect inboard of the subduction of the Cocos Ridge is the indentation of the frontal part of the upper plate accompanied by landward shift of the trench. It remains a matter of

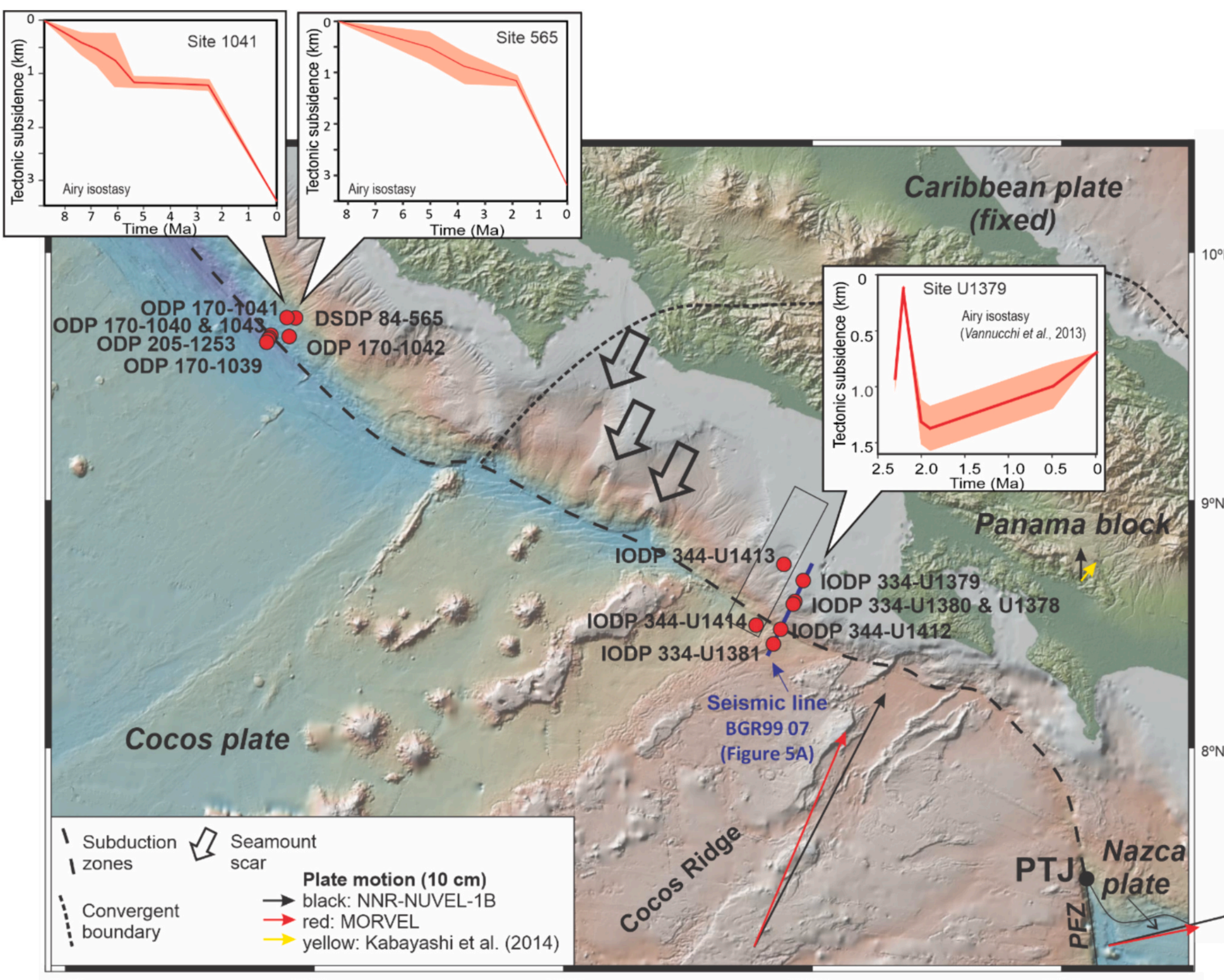

Fig. 4. Digital elevation and bathymetry of the Middle America Trench offshore Costa Rica – plate tectonic velocities have been calculated according to NUVEL-1B (DeMets, 2001) and MORVEL (DeMets et al., 2010; Argus et al., 2011) with geodetic estimation for the Panama block (Kobayashi et al., 2014). Insets show the published tectonic subsidence curves for sites offshore the Nicoya Peninsula and the Osa Peninsula (Vannucchi et al., 2003b; Vannucchi et al., 2013). In this map the traces left on the forearc by subducting seamounts are visible.

debate whether this retreat is the result of net material loss (Vannucchi et al., 2013), underthrusting of the outer forearc beneath the inner forearc (Morell et al., 2019) or is simply not present (Edwards et al., 2018).

4.1. Ocean drilling data

In Southern Costa Rica IODP Exp. 334/344 drilled the northwestern flank of the subducting Cocos Ridge and cored the forearc material from the incoming plate to the shelf along two transects ≈12 km apart (Vannucchi et al., 2012; Harris et al., 2013). The NW transect lies within a 3D seismic reflection volume (Bangs et al., 2015) coincident with the path of a subducting seamount present on the flank of the Cocos Ridge (Kluesner et al., 2013; Martinez-Loriente et al., 2019).

The sedimentary succession of the incoming plate drilled on the Cocos Plate at Sites U1381 (8.42858, −84.15781) and U1414 (8.50384, −84.22549) consists of Miocene biogenic pelagic sediments, i.e. calcareous oozes, overlain by Miocene to Pleistocene hemipelagic silty clays (Fig. 5). Drilling and sampling at Site U1412 on the forearc toe (8.48599, −84.12918) revealed a stack of Cocos plate hemipelagic and pelagic sediments that were transferred at the front of the Caribbean plate (Harris et al., 2013) in agreement with reflection seismic profiles that show a 5 to 10 km wide accretionary prism (Arroyo et al., 2014). Despite not reaching the decollement, Site U1412 cored a former frontal thrust with the Miocene calcareous oozes thrusted on top of the younger Pleistocene silty clays (Harris et al., 2013). This geometry reveals that the megathrust cuts into the calcareous pelagic sediments (Vannucchi et al., 2017). Initially, the location of the megathrust within the pelagic sediments was independently confirmed by the interpretation of 3D seismic data (Bangs et al., 2015). However, a subsequent analysis of the same seismic survey obtained a contradictory determination (Edwards et al., 2021). The revised interpretation shifted the megathrust's location to lie within the hemipelagic sediments, diverging from the indications obtained through drilling. Based on the microfossil content of the footwall sediments of the drilled thrust, accretion trenchward from Site U1412 occurred within the last ~1.9 Myr (Harris et al., 2013).

Moving landward, reflection seismic images of southern Costa Rica forearc show that a high-amplitude reflector marks the base of forearc sediments, similar to what is also imaged in the Japan Trench forearc. The reflector, which appears as an angular unconformity, was drilled and sampled at both Sites U1379 and U1380.

Site U1379 is located on the shelf/upper slope in 125 m-deep water,

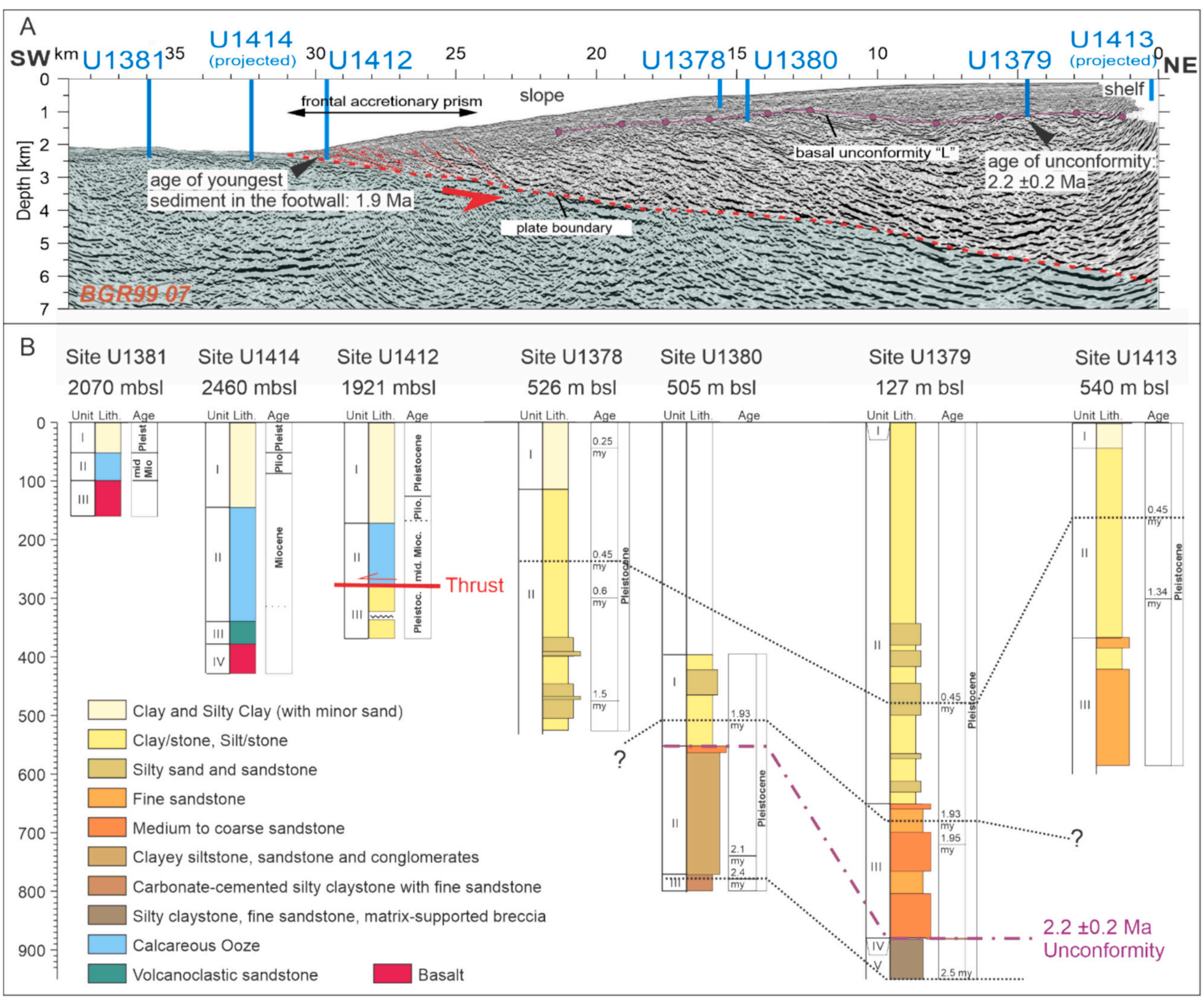

Fig. 5. (A) IODP Exp. 334 and 344 drill site locations shown on BGR99 07 seismic reflection line (Arroyo et al., 2014)]. Line location is shown in Fig. 4. The shaded green area denotes the subducting plate. The high-amplitude reflector at the base of the slope sediments is marked by blue dots. (B) Stratigraphic summaries of CRISP sites. Solid black lines correlate the same ages between sites. The purple dash-dotted line correlates the basal unconformity between Sites U1379 and U1380. The red solid line at Site U1412 marks the repetition of ages interpreted as a thrust. The incoming plate sites U1381 and U1414 were drilled in a basement high and basement low, respectively.

≈ 34 km offshore Osa Peninsula (8.68083, −84.03361). Drilling recovered ~100% of a thick sequence of poorly deformed terrigenous sediments, and penetrated the unconformity responsible for the high amplitude reflector at ≈880 mbsf. It also cored 80 m of still poorly deformed fine to coarse-grained volcanoclastic turbidites, hemipelagites, and megabreccias that underlie the unconformity. These older sediments are typical of a deep-water environment and have been dated to the early Pleistocene ~2.5 Ma (Calcareous nannofossil zone NN18–17)(Vannucchi et al., 2012; Vannucchi et al., 2013; Schindlbeck et al., 2016). The unconformity, dated at 2.2 ± 0.2 Ma, does not present a hiatus that is detectable with micropaleontological dating (Vannucchi et al., 2013; Schindlbeck et al., 2016). Its occurrence is instead marked by a sharp lithostratigraphic change to a < 2 m-thick carbonate cemented sandstone bearing shell fragments and basaltic pebbles (MORB type). This sediment was interpreted to indicate a beach/near-shore depositional environment accompanied by mud cracking that implies subaerial exposure (Vannucchi et al., 2012; Vannucchi et al., 2013) (Fig. 5).

At Site U1380 (8.59992, −84.08318), located ≈10 km downslope from Site U1379, the high amplitude reflector corresponds to an 11-m-thick deposit now located at ≈550 mbsf. This deposit consists of shell-rich sand/stone layers alternating with few clayey siltstone layers (Harris et al., 2013). Sedimentation appears linked to reworking of material deposited upslope. However porosity profiles and zeolite assemblages at Site U1380 argue for ≈300 m of sediment having been removed above the reworked sand in ≈ 0.5 Ma (Hamahashi et al., 2017). At Site U1380 the unconformity appears younger than at Site U1379, however precise dating has been challenging. Micropaleontological analyses placed at 510 mbsf the limit between NN18 e NN19 (nannofossil zones), i.e. 1.93 Ma (Harris et al., 2013). This age is confirmed by magnetostratigraphy (Xu et al., 2021) and agrees with tephrachronology (Schindlbeck et al., 2016), which consistently imply an age of ~2 Ma for the unconformity at Site U1380 (Vannucchi et al., 2016b).

Finally, the shelf was drilled at Site U1413 (8.74098, −84.11349), ca. 15 km to the NW of Site U1379, where coring reached ≈580 mbsf without penetrating the unconformity that marks the base of the forearc sediments (Fig. 5). At Site U1413, biostratigraphy indicates ages of 0.45 Ma at a depth of ≈160 mbsf (top of NN19) and 1.34 Ma at ≈300 mbsf (Harris et al., 2013). Additionally magnetostratigraphy dates the sediments recovered at ≈380 mbsf at 1.82 Ma (Xu et al., 2021). The deepest recovered samples are dated to be ≈2.5–2.7 Ma (Schindlbeck et al., 2016), which suggests that drilling at Site U1413 almost reached the base of forearc sediment unconformity.

Further analyses on the benthic fauna assemblages preserved at the shelf/middle slope sites reveals the vertical tectonic evolution of the forearc. Above the erosive subaerial unconformity at Site U1379 the forearc sediments record a short (<2 Myr) interval of extreme subsidence (≈1200 m) with rapid sinking occurring during the first ≈0.3 Myr, followed by relative uplift to the modern depth (Fig. 4) (Vannucchi et al., 2013). The sedimentation rate in the forearc basin was rapid, with a peak in the last 0.6 Ma where it reached 1035 m/Ma (Vannucchi et al., 2016b). Sites U1380 and U1413 confirm the general trend of vertical movements of the forearc recorded at Site U1379 (Vannucchi et al., 2016a).

4.2. Seismostratigraphic interpretation of the forearc basin

The forearc basin imaged with 3D reflection seismics was interpreted using a seismostratigraphic approach (Edwards et al., 2018). This analysis highlighted i) a history of vertical movements of the forearc inferred by the presence of laterally continuous unconformities, and ii) a stable position of the shelf break throughout the Pleistocene.

Site U1413 lies within the 3D reflection seismic volume and so can help to unravel the evolution of the forearc basin. The analysis of the seismic data suggests that the unconformity at the base of the forearc sediments – called "L" which in this area should be dated at 2.3–2.5 Ma - ranges from 850 to 2900 mbsf, with an inferred depth of ≈2000 mbsf at Site 1413 (Edwards et al., 2018). Two other shallower unconformities were also interpreted within the forearc sediments and over a laterally continuous area (Fig. 6) (Edwards et al., 2018).

- An intermediate "M" unconformity located at ≈500 mbsf, which corresponds to sediments of ≈ 1.95 Ma at Site U1413 (Xu et al., 2021). It extends from the shelf to within 5–10 km from the trench, and appears pervasively channelized with steep downcutting and total surface erosion that reached 900 m in the middle slope. These characteristics suggest that the unconformity is likely to be the result of a major slope collapse that removed a thick section of the wedge.
- An upper "U" unconformity located at ≈180 mbsf extends from the shelf to ≈ 5 km from the trench and is given an age of 1.19–1.78 Ma. It is parallel to the present-day seafloor and relatively smooth with short channels intersected by small offset normal faults. The ≈180 mbsf unconformity is interpreted to be formed by subaerial erosion (Edwards et al., 2018).

Unfortunately neither visual core description, physical properties, or the age at Site U1413 confirm the presence of these unconformities at ≈500 mbsf and at 180 mbsf at Site U1413, except for a change in benthic foraminifera assemblage that occurs at ≈500 mbsf (Harris et al., 2013). While this lack of evidence in the cores might be due to a local "para-conformity" nature of these surfaces, if these unconformities exist, they are not calibrated regarding either their nature or their age. Therefore, based on drilling results, the penetration of two possible extensive unconformities at ≈500 mbsf and at ≈180 mbsf at Site U1413 remains unsupported. In the same way the interpretation of the two unconformities as marking uplift or even subaerial erosion is also unsupported by drilling results. Moreover no benthic foraminifera analysis for paleodepth was conducted at this site due to the essentially barren nature of the sediments (Harris et al., 2013), and paleodepth interpretations were possible only through sedimentological analyses, which prevent a detailed analysis of their vertical movement. Notably, the sediments recovered at Site U1413 do not indicate subaerial events, and, unlike the seismostratigraphic interpretation of seismic images that describes a sedimentation environment marking major slope collapse at depths corresponding to ≈500 mbsf (Edwards et al., 2018), the sediments drilled at Site U1413 recovered mass transport deposits only above ≈150 mbsf (Harris et al., 2013). Finally tephrachronology and magnetostratigraphy dated the sediments recovered at the bottom of Site U1413, ≈580 mbsf, to be 2.5–2.7 Ma old (Schindlbeck et al., 2016; Xu et al., 2021) implying that the base of the forearc sediments is within a few tens of m below the bottom of the site, and not at 2000 mbsf as inferred by the seismostratigraphic interpretation. Problems also arise with the inferred seismostratigraphic age of the ≈180 mbsf unconformity. According to the seismic interpretation this should correspond to a 1.19–1.78 Ma event (Edwards et al., 2018), but analyses of the sediments recovered at ≈180 mbsf indicate ages of ≈ 0.44 Ma (Vannucchi et al., 2016b; Xu et al., 2021). This intercomparison between the seismostratigraphic interpretation and the age and nature of sediments recovered in the forearc basin highlights problems in the reconstruction of the Pleistocene vertical movements based on inferences from only seismic data.

A second issue regards the evolution of the shelf break. The inner/outer wedge transition is approximately consistent with the shelf break (Fig. 6).

In the 3D seismic data the inner wedge, broadly corresponding to the shelf portion of the forearc characterized by limited visible compressional deformation is clearly distinguished from the outer wedge, corresponding to the folded and thrusted slope portion (Bangs et al., 2016). This indicates that the shelf break is a key marker for the transition between different structural domains within the forearc. One of the main inferences drawn from this is that the inner/outer wedge transition did

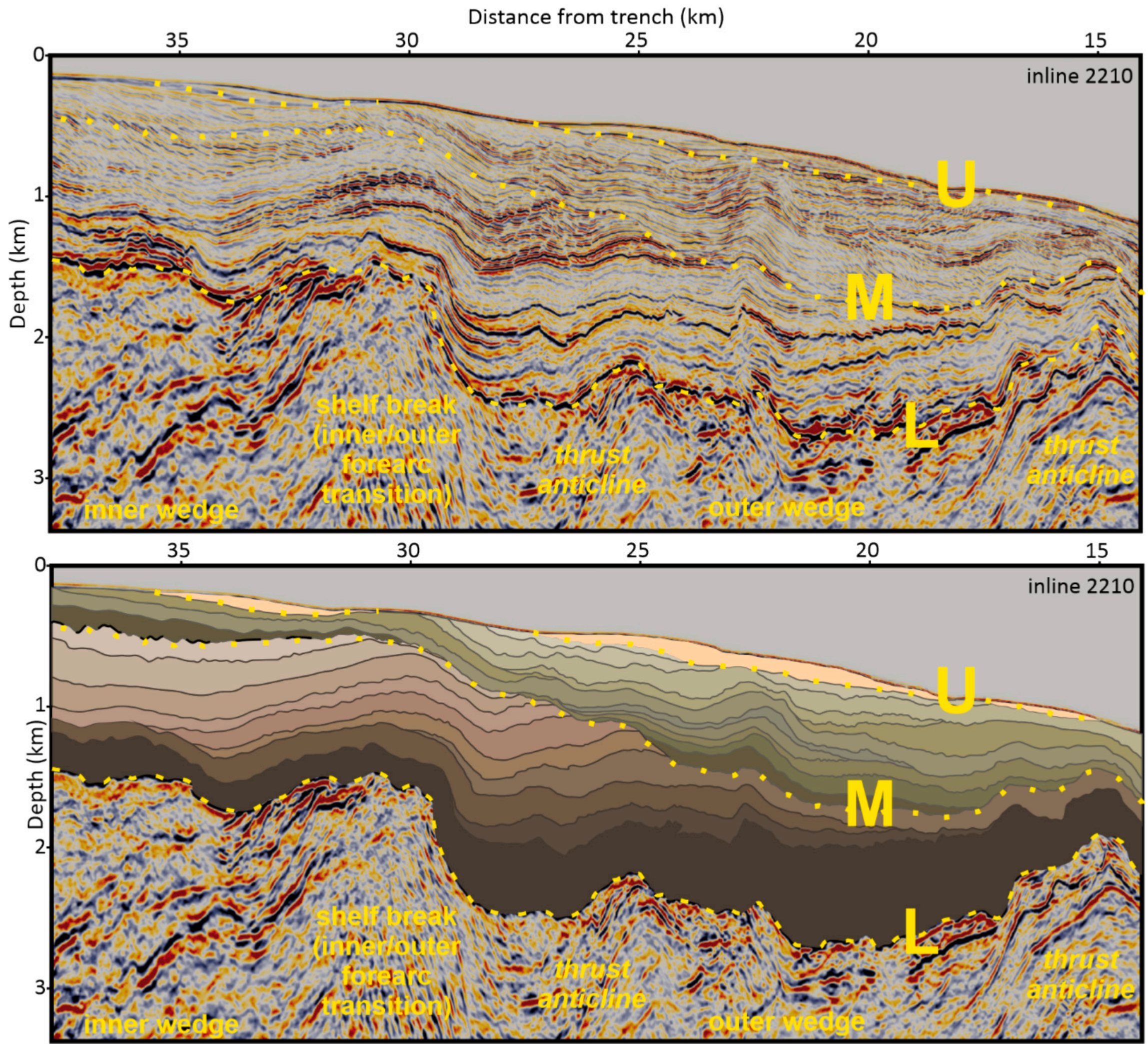

Fig. 6. Seismic section acquired within the 3D seismic reflection box (location in Fig. 4) modified from Edwards et al. (2018). This figure shows uninterpreted (top) and interpreted stratal domains, erosional events, and depositional sequences from the outermost shelf down to the middle slope. Vertical exaggeration is 3 for all figures.

not migrate relative to the forearc throughout the Pleistocene, i.e. above the high-amplitude reflector marking the base of the forearc basin (Edwards et al., 2018). Assuming that, if tectonically eroded, the forearc would reshape to reach a stable profile, the absence of migration of the shelf break would imply absence of trench retreat, i.e., this would be an argument against basal erosion being active through the Pleistocene. Edwards et al. (2018) instead suggest that the vertical motions of the Costa Rican outer forearc are the result of episodic events such as the passage of the Panama Triple Junction and seamounts that induced margin shortening.

However, in the seismostratigraphic interpretation presented in Fig. 6, it is evident that the sedimentary deposits located between the base-of-forearc-basin "L" unconformity and the intermediate "M" unconformity grow thicker towards the trench side of the proposed stable inner/outer forearc transition. This observation would strongly imply that the landward side of this transition experienced less sediment deposition than its trenchward region which functioned as an older major depocenter with characteristics of a forearc basin. In this case the forearc basin, and therefore the shelf break, would have indeed migrated to its present position beneath the continental shelf. The unconformities highlighted by Edwards et al. (2018) prominently reveal extensive erosion of older strata, introducing uncertainties concerning the precise positioning of the inner/outer forearc during the critical period around 2.2 Ma ago. Additionally, the base of the slope sediment reflector appears to have been deformed by thrusting processes. If subducting bathymetric relief triggered margin shortening, this would in turn cause the progressive landward shift of the shelf-slope break, a well-known effect in an imbricated system of thrusts (Karig and Sharman, 1975). A rapid pulse of subduction erosion (ca 200 k yrs), instead, would not leave the time for the margin to adjust to the new configuration and would remove lower slope material while maintaining almost "intact" the shelf-upper slope region, that would undergo mostly uplift and subsidence.

These issues highlight problems in assuming that the shelf break did not migrate relative to the forearc since the early Pleistocene, and affects some of the models that reconstruct the evolution of the margin (Edwards et al., 2018; Morell et al., 2019; Edwards et al., 2021).

4.3. *The nature of the forearc: The accretionary prism hypothesis*

Landward of the ~1.9 Ma old frontal accretionary prism and below the 2 ± 0.2 Ma old forearc slope/shelf unconformity the nature of the forearc has been investigated through drilling and seismic imaging. The sediments recovered at Site U1379 and U1380 below the base of the forearc sediment unconformity are deep water hemipelagic sediments with microfossil fauna that differ from those recovered in the sediments of the incoming Cocos plate that indicate abyssal water depths - >2000 m – (Harris et al., 2013; Vannucchi et al., 2013; Vannucchi et al., 2016b). At Site U1379 the hemipelagic sediments below the unconformity alternate with sedimentary breccias indicating possible mass flow deposits. Also, below the unconformity the sediments recovered at Site U1379 and U1380 are undeformed. In fact at both sites deformation – mesoscopic faults and tilted beds – is concentrated in the sediments above the unconformity (Vannucchi et al., 2012; Harris et al., 2013). This finding is in contrast with the jump in deformation intensity anticipated for an accretionary prism where relatively undeformed sediments of the slope apron should lie on top of more deformed sediments of the accretionary prism (Lundberg and Moore, 1981; Hayman et al., 2012).

Reflection seismic images, including those from the 3D volume, show an outer forearc characterized by a layered fabric consistent with clastic sediments, and landward dipping reflections interpreted as thrusts, folds, and high angle normal faults (Bangs et al., 2016). In general the wavelength of folding decreases from the inner wedge towards the trench (Bangs et al., 2016; Vannucchi et al., 2016b) while the extensional faults are mostly limited to the topmost part of the forearc (Kluesner et al., 2013).

The outer forearc landward of the frontal accretionary prism has been interpreted to have evolved following either an accretionary model (Bangs et al., 2016) or a 'depositionary" model (Vannucchi et al., 2016b). The accretionary model focuses on the geometry that reproduces imbrication of stacked thrust packages. These packages are thicker and with greater spacing moving landward (Bangs et al., 2016; Martinez-Loriente et al., 2019) possibly reflecting a period when trench deposits were thicker than today. Bangs et al. (2016) inferred that the passage of the Panama Triple Junction (Cocos-Nazca-Caribbean) could have increased the amount of sediment delivered to the trench by causing a collapse of the frontal part of the forearc, similar to what is visible today between the Coiba Ridge and the Panama Fracture Zone (PFZ). Considering that the PFZ is now ≈150 km from the CRISP area, and that the Panama Triple Junction is migrating to the SE at a rate of 30–55 mm/yr depending on the plate velocity model (McIntosh et al., 1993; Sitchler et al., 2007; Morell, 2015), the sediments would have been delivered to the trench and accreted between 5 and 2.7 Ma (Fig. 7). This age is older/overlapping with the onset of subduction of the Cocos Ridge in the CRISP area, whose western boundary there was the Panama Triple Junction itself. Typically the subduction of an aseismic ridge would lead to a deep indentation in an accretionary prism, and temporarily inhibit the accretion of new sediments (Dominguez et al., 1998). Therefore, if the sediments delivered to the trench were already accreting, ridge subduction would have swept away the prior accretionary prism. Furthermore these thrust packages have decreasing offsets landward, a feature that according to some authors makes them consistent with the accretionary model (Edwards et al., 2018) despite the observed landward increase in finite strain.

Following the accretionary scenario, we can also perform a mass balance for this margin. In an accretionary-type margin the age of the base of forearc sediment unconformity, which seals the accreted thrust packages and therefore marks the age of accretion, should decrease trenchward. Thus, trenchward of Site U1379 tectonic accretion would be inferred to be younger than 2.2 ± 0.2 Ma. It is important to note that within the framework of the accretionary prism model, the material beneath the unconformity is considered as accreted, rather than having been part of an ancient forearc basin. Site U1412, located at the forearc toe, indicates that any accretion occurring landward of this point is older than ≈1.9 Ma. Within these limits, the margin wedge should have been accreted between ≈2.4 and ≈1.9 Ma.

In the velocity diagrams black lines refer to velocities of Cocos (CO) and Nazca (NZ) with respect to Caribbean (CA), blue lines refer to velocities of CO and NZ with respect to Panama (PM) and of PM to CA, dashed red lines represent the orientations of the PFZ and MAT, solid red line is the orientation of the Cocos Ridge axis inferred from Fig. 4. Intersection of MAT and PFZ is PTJ.

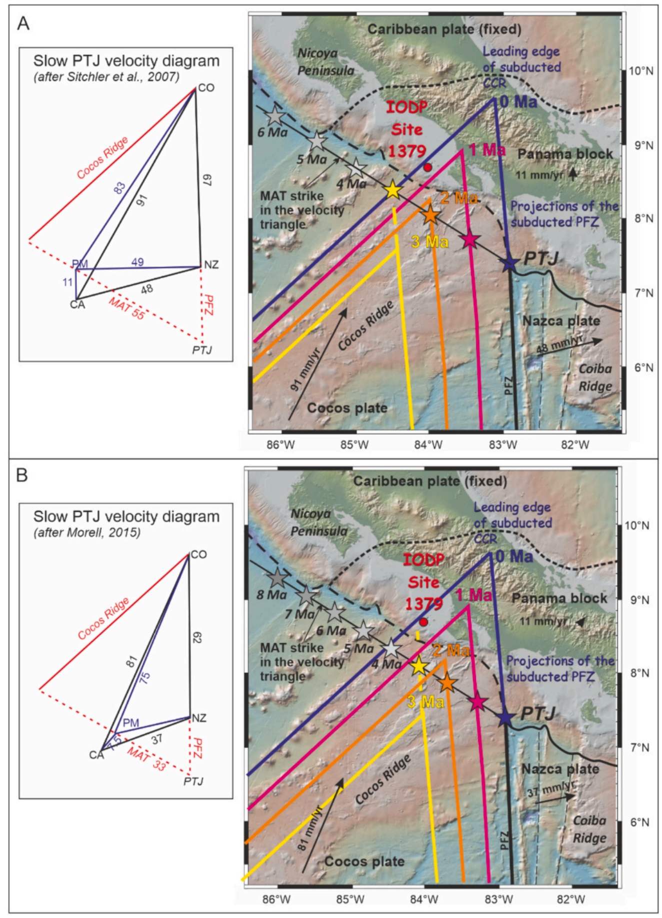

Fig. 7. Reconstructed migration of the Panama Triple Junction (PTJ) and Cocos Ridge through time given two different velocity models: A) a "fast" velocity model (Sitchler et al., 2007), modified for the orientation of the Cocos Ridge axis striking at 45°, based on NNR-NUVEL-1B plate velocity model (DeMets et al., 1990) and estimates from Bird (2003) regarding the Panama block; and B) a "slow" velocity model (Morell, 2015), modified for the orientation of the Cocos Ridge axis striking at 45°, based on MORVEL plate velocity model (DeMets et al., 2010; Argus et al., 2011) and estimates from Kobayashi et al. (2014) regarding the Panama block. Stars refer to PTJ location through time along the Middle America Trench (MAT) strike. Geometry of Cocos Ridge reconstructed assuming a simple projection of the Panama Fracture Zone (PFZ) to the north and the NW edge of the Cocos Ridge to the NE.

Considering the relative position of Sites 1379 and 1412, the volume of material accreted should have been 80 km^3 per km of trench at a rate of ~400 km^3/Ma per km of trench. Assuming a Pleistocene convergence rate similar to the current rate of 90 mm/yr, the sediment column on the incoming Cocos plate should have been ~3 km thick (varying between 9 km if the unconformity is 2 My and 2 km if the unconformity is 2.4 my) – without correcting for compaction – which is comparable to the sediment thickness of some of the most sediment-rich trenches in the world (Olsen et al., 2020).

Today, the PFZ is responsible for a ≈ 50 km wide area of topographic relief where the average difference in height is of ≈1 km. Therefore, the Panama Fracture zone could not have contained a 3 km-thick sediment fill. Moreover, the sediment fill in the PFZ itself is ≈ 300 m on average (Whittaker et al., 2013) in agreement with the sediment fill of the nearby Ecuador Fracture Zone (Kolandaivelu et al., 2017).

An alternative model to the accretionary prism considers that the sediments under the unconformity once formed part of an older forearc basin (Vannucchi et al., 2012; Vannucchi et al., 2013; Vannucchi et al., 2016b). In the depositionary model the outer forearc landward of the frontal prism is formed by terrigenous sediments that accumulated in response to oversteepening of the margin due to the onset of Cocos Ridge subduction. This model was built using the observation of an exceptionally high recent sedimentation rate of forearc sediments that peaked in the last 0.6 Ma at a rate of 1035 m/Ma (Vannucchi et al., 2012; Vannucchi et al., 2016b).

4.4. Discussion

Before investigating the processes that might have shaped the southern Costa Rica subduction margin, it is useful to review the motivations and data that drive some recent models.

As an alternative process to subduction erosion, the process responsible for subsidence of the outer forearc has been recently linked to shortening and thickening (Edwards et al., 2018; Morell et al., 2019). Note that potential large-scale subsidence induced by shortening in southern Costa Rica is strikingly different from the extension-induced subsidence proposed to have taken place in the Japan forearc (Edwards et al., 2018). The concept of compression-induced subsidence, moreover, is at odds with fundamental principles of isostasy. Extension- and contraction-induced subsidence have been associated to changes in the geometry of an elastic shallow slab (Regalla et al., 2013; Edwards et al., 2018). However, both the incoming Cocos plate offshore Costa Rica and the Pacific plate offshore Japan are characterized by bend-faulting (Ranero et al., 2003; Fujie et al., 2018) and seismic datasets show that the subducting slabs fail throughout the depth-interval below the outer forearc (Ranero et al., 2005; Obana et al., 2012; Lucke and Arroyo, 2015). An elastic- perfectly plastic behavior of the bending slab, i.e. after the plate enters the subduction system, was already preferred in the plate subduction models proposed in the late '70ies (Turcotte et al., 1978), even before the discovery of bend faults in the outer rise of the incoming plate. Finally, while elastic flexural bending can be used to model the fore-bulge on the incoming plate, plastic and viscous models have also been used to quantitatively fit fore-bulges with the possibility of a contribution from bend faulting (Morgan and Ranero, 2023).

4.4.1. Cocos Ridge subduction

The chain of events that shaped the vertical tectonic evolution of the southern Costa Rica forearc has been variously interpreted using the subsidence/uplift curve determined from Site U1379 (Fig. 4) (Vannucchi et al., 2013). This curve is also consistent with the early Pleistocene age of the outer forearc subsidence offshore Nicoya Peninsula – about 200 km to the NW of Osa Peninsula – where rapid subsidence occurred in two separate events: at ~6 Ma and at ~2–2.5 Ma (Vannucchi et al., 2003a; Vannucchi et al., 2016a). The record of simultaneous widespread deformation along the margin is consistent with plate tectonics reconstructions for the onset of Cocos Ridge subduction which indicate ages between 2 and 3 Ma (Morell et al., 2011; Morell et al., 2019). As an alternative, the transient uplift of the slope and shelf offshore Osa Peninsula has been attributed to the SE migration of the Panama Triple Junction along the margin (Edwards et al., 2018; Morell et al., 2019; Edwards et al., 2021). Notably geometrical constraints suggest that the triple junction migration through southern Costa Rica is intrinsically connected to the onset of subduction of the Cocos Ridge, as the PFZ here truncates the Cocos Ridge and forms its eastern boundary. This tectonic juxtaposition likely intensified the sharp bathymetric changes associated with the PFZ, further amplified by the Cocos Ridge's presence to the west. Assuming a past geometrical relationship consistent with the present one, the Cocos Ridge would have indented the margin like a "keel" (Fig. 7) leading to a relatively small, subducted portion of the ridge beneath the Osa Peninsula— ≈ 200 km — that has steep lateral boundaries. Additionally, the SE triple junction migration at a rate of ≈30–55 km/yr (McIntosh et al., 1993; Sitchler et al., 2007; Morell, 2015), is consistent with the subsidence event recorded offshore the Nicoya Peninsula at ≈6 Ma (Fig. 7)(Vannucchi et al., 2016a).

All authors acknowledge that subsidence across the shelf implies significant thinning of the margin wedge, however a key difference in the proposed models resides on the processes responsible for thinning – and the amount of thinning.

One model put forward by Edwards et al. (2018) suggests that forearc thinning is achieved by subaerial erosion of at least 500 m of sediments. Subsidence would then follow due to the continued SE migration of the PFZ triple junction, which not only had associated bathymetry, but also drove a replacement of the Nazca plate slab with the Cocos plate slab, that is proposed to accommodate ≈2000 m of extra subsidence (Edwards et al., 2018). In this model, not only does this replacement affect the convergence rate perpendicular to the margin, which increased from ≈20 mm/yr to ≈80 mm/yr (Morell, 2015), but it also changes the crustal thickness of the subducting slab. A bigger downward flexing of the Cocos slab, inferred to be thinner than the Nazca slab, is potentially invoked under the outer forearc as a mechanism to decrease the radius of slab curvature or drive negative slab buoyancy with the final result of gaining room for the forearc basin with its very high sedimentation rate (Edwards et al., 2018). However geophysical studies indicate ca. 7–10 km thick crust for both the Cocos and the Nazca plates outside of the Cocos Ridge that bears the only crustal thickness anomaly in this region – between ≈16.5–19 km (Sallares et al., 2003). Margin wedge thinning by subaerial erosion is at best weak in its first principle, while subsidence driven by change in slab crustal thickness is not supported by geophysical data. Notably the opposite argument – thick and relatively shallow Cocos Ridge slab – is often proposed as the driver of the shortening and thickening of the margin wedge (Morell et al., 2019).

An alternative scenario for margin wedge thinning considers the response of a forearc to underthrusting bathymetric highs and the damage produced on the wedge itself which must deform to allow for variations in the incoming plate geometry. The presence of a topographic perturbation on the footwall of a thrust would promote failure in the hanging wall (Knipe, 1985). The subduction of a topographic high, such as a seamount, is known to promote failure of the overriding plate (Dominguez et al., 2000; Wang and Bilek, 2011). Increased tectonic loading on the leading flank of the subducting seamount would also lead to large deviatoric stresses (Sun et al., 2020), while displacement over these features imposes a deformation rate on the megathrust that can be reduced by generating cutoffs on the overriding plate (Knipe, 1985) already weakened by failure. This process can result in local basal erosion of the upper plate material, as indicated by the scarring patterns observed on the outer slope of forearcs impacted by seamounts (von Huene et al., 2000). In this scenario upper plate thinning occurs "from below" with subsidence of the upper plate being a direct consequence. Thinning of the upper plate occurs while both compression on the leading flank of the subducting seamount and the subducting relief are causing total uplift of the forearc (Fig. 8).

Unlike a subducting seamount, an aseismic ridge that is subducting sub-perpendicular to the margin is a stationary high relief and thick crustal feature. The first big difference between the effects produced by a subducting seamount or a ridge is that through time the ridge is predicted to push the forearc material radially away from its frontal part with the result that compression is present in front of the ridge and along its flanks and extension prevails above the ridge tip (Zeumann and Hampel, 2015). Extension would cause a pulse of relative subsidence behind the ridge tip followed by a second, slower phase of uplift (Zeumann and Hampel, 2015). This trend well describes the evolution of the subsidence/uplift curve from Site U1379 to its present state.

In other scenarios the Cocos Ridge subduction is viewed as having led to far less disruption than subduction of a few seamounts (Edwards et al., 2018). In fact after passage of the triple junction the following subsidence/uplift events predicted by the reflection seismic interpretation, although not shown in the drilling record, would have formed by a seamount subduction event at ≈1.8 Ma, and a "plateau" subduction event at ≈1.3 Ma, which would carry a topographic relief that is more than twice as large as the Cocos Ridge (Edwards et al., 2018).

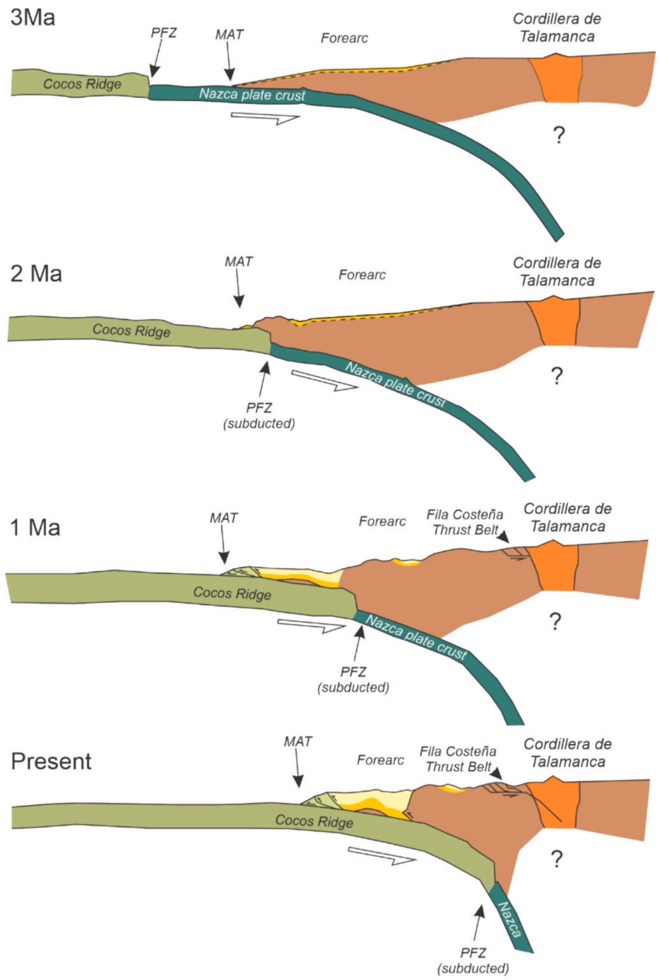

Fig. 8. Evolution of Cocos Ridge subduction from 3 Ma to Present following the spatial progression suggested in Fig. 7.

In summary, this proposed reconstruction has several concerning issues: (a) It has a basic issue in that a subducting seamount is proposed to lead to far more damage to the overriding plate than the subduction of a sharp deep fracture zone immediately followed by the onset of subduction of a ~ 2 km high oceanic plateau; (b) It misdates several key events based on incorrect readings of Site U1439 data; (c) Its Pleistocene tectonic setting offshore southern Costa Rica also seems flawed.

4.4.2. Trench Retreat

Arcward retreat of the trench (movement of the trench towards the direction of the volcanic arc) also occurs during the indentation of the forearc by the subducting Cocos Ridge. Inboard of the indentation and at the back of the Osa Peninsula, the inner forearc is characterized by the formation of a fold-and-thrust belt that forms the Fila Costeña mountain range. The Fila Costeña extends for 200 km, inshore of the Cocos Ridge on the incoming plate, with its maximum development corresponding to the offshore axis of the Cocos Ridge, and decreasing symmetrically to the northwest and southeast of this axis. Interestingly the Fila Costeña is a thin-skinned belt that deforms the sediments of a Miocene/Pliocene basin while leaving the Caribbean forearc basement below the basal decollement undeformed within the thrust belt (Fig. 8) (Fisher et al., 2004; Sitchler et al., 2007; Morell et al., 2019).

The Fila Costeña is a unique feature along the Central America forearc. Although its onset time is debated, with some authors ascribing it to the Miocene and others to the Pliocene (Morell et al., 2019 and ref. therein), its development appears to be linked to the forearc retreat and shortening induced by Cocos Ridge subduction. In fact, the enhanced compression is anticipated at the downdip leading edge of subducting topography in analog and numerical experiments (Zeumann and Hampel, 2015; Zeumann and Hampel, 2016; Sun et al., 2020).

Morell et al. (2019) propose that the retreat of the trench towards the arc is directly linked to compression in the Fila Costeña, and that forearc shortening occurs through underthrusting where the outer forearc is pushed beneath the inner forearc. Consequently, the basal thrust of the fold-and-thrust belt would separate an internally deformed hanging wall, consisting of the inner forearc, from a less internally deformed footwall, composed of the outer forearc, given the thin-skinned nature of the Fila Costeña. This tectonic edifice would overlay or be positioned at the forefront of the subducting Cocos Ridge, while the outer forearc is not yet underthrust, so it would experience primarily transient rapid vertical tectonic movements due to the subduction of the irregular bathymetric relief associated with the Cocos Ridge and Panama Fracture Zone. Although these authors argue that the subduction of the Cocos Ridge occurs without tectonic erosion of the forearc, underthrusting implies the removal of the frontal part of the forearc and therefore frontal erosion of the upper plate. Moreover, Morell et al. (2019) do not offer a mechanism for how the Cocos Ridge subduction would cause differential shortening within the outer and inner forearc. In fact, numerous field observations (von Huene and Scholl, 1991; Kopp, 2013), laboratory analogue experiments (Dominguez et al., 2000; Martinod et al., 2013; van Rijsingen et al., 2019), and numerical modeling (Ding and Lin, 2016; Ruh et al., 2016; Morgan and Bangs, 2017; Sun et al., 2020) indicate that subducting topography can significantly fracture the upper plate as a whole and disrupt its stratigraphy.

The effects of the subducting ridge topography on the forearc have been invoked to account for the rapid (>1 m/kyr), brief (<1 Myr) pulses of uplift and subsidence observed in the forearc, which exhibit spatial irregularity over distances of <10 km. This "yo-yo" tectonics is strongly manifested in the Osa Peninsula, where its ups and downs correspond to the topographic highs and lows along both the crest and flanks of the Cocos Ridge/PFZ (Fisher et al., 1998; Sak et al., 2004; Vannucchi et al., 2006). These secondary tectonic events are superimposed on a primary event that is characterized by the initiation and ongoing subduction of the Cocos Ridge, which also resulted in a brief (<0.2 Myr) episode of uplift and subsidence along the margin (Vannucchi et al., 2013).

5. Conclusions

This paper highlights the complexity of forearc evolution at subduction zones. Multiple competing models have been proposed to interpret and explain the observed local geological features at different forearcs. This complexity likely reflects the dynamic interaction of various tectonic processes operating within subduction zones. Key questions revolve around material transfer between the subducting and overriding plates, encompassing subduction, accretionary prism formation, and tectonic erosion. Table 1 synthesizes the proposed alternative models to subduction erosion and their counter arguments. Table 1 also includes references to the concerned periods in the two chosen trenches, since each process may be active at a given moment in the tectonic evolution of the margin.

Forearc subsidence has been often linked to upper plate thinning by tectonic erosion occurring both at the front or at the base of the forearc. However, forearc thinning mechanisms are debated with alternative models to subduction erosion such as extensional tectonics, subaerial erosion of sediments and changes in slab geometry. While the last two models do not agree with first principles of isostasy, extensional tectonics fails to provide a quantitative solution for observed forearc volumes in the Japan Trench forearc and would require subsequent subduction erosion to account for observed subsidence patterns.

Subduction of topographic relief has long been recognized as a mechanism that causes forearc thinning and localized subduction erosion, although recently it has been proposed as a mechanism driving net accretion to the margin. Accretion would happen at depth and would

Table 1
Summary of arguments proposed as alternatives to tectonic erosion and their counter-arguments.

Proposed alternative model to tectonic erosion	Place and period concerned	Counter-argument
Extensional Tectonics. Forearc thinning and subsidence can be achieved by extension linked to normal faulting.	Japan - Oligocene to Present.	- Mass balance calculations indicate that observed forearc subsidence cannot be achieved by normal faults, which lack sufficient number and/or displacement to support lithospheric thinning.
Isostatic Adjustment. If tectonic erosion removes not only low-density forearc crust, but also high-density material from the mantle wedge, it should cause uplift.	Japan - Oligocene to Present.	- Because the eroded crustal material is replaced by even denser mantle beneath the subducting crust, the expected uplift does not occur. Even if mantle wedge material was eroded it too would be replaced by denser mantle beneath the subducting crust, so this too would not lead to isostatic uplift. In addition, the constant thickness of the subducting oceanic crust does not impact the isostatic calculations, so its effects can be disregarded.
Steady-state forearc – no-net accretion and full sediment subduction. Forearc thinning and subsidence can be achieved by lack of sedimentary buildup due to full sediment subduction.	Japan - Oligocene to Present.	- Mass balance calculations indicate that the volume of the forearc wedge is too small to account for a stable forearc. This would lead to an unrealistic profile of the forearc wedge itself.
Plate Kinematic change. Subsidence caused by changes in shallow slab geometry. If plate convergence increases, the effective elastic thickness (Te) of the slab increases and therefore the slab would bend at a higher radius of curvature. In turn the horizontal movement of the slab within the upper part of the mantle can be made more difficult resulting in a seaward retreat of the trench which would create extra space allowing back-arc spreading and forearc subsidence.	Japan - Oligocene to Present.	- Geophysical data indicate that the subducting slab fails throughout the depth-interval below the outer forearc, even at the trench and at shallow depths where bend faulting is widespread, questioning the elastic behavior of the slab. - Depending on thermal structure and composition of the slab, higher convergence rates could simply cause more brittle failure and higher plastic deformation rather than an increase in Te. - Higher convergence rates and slab shallowing can lead to increased compressive forces, potentially thickening the lithosphere and leading to uplift rather than subsidence.
Forearc shortening (1). Forearc subsidence would be achieved by flexural response to loading.	Middle America Trench (SE Costa Rica) – Plio-Pleistocene to Present	- Horizontal compression typically results in crustal thickening which would lead to isostatic uplift. - Isostatic adjustments often lead to rebound and uplift rather than long-term subsidence, counteracting the initial subsidence caused by flexural loading. - The slab could be too strong or too thick to flex significantly. - If the slab is buoyant or strongly coupled to the forearc, subducting topography may actually push the forearc upward rather than allowing it to flex downward.
Forearc shortening (2). Subduction of an aseismic ridge (Cocos Ridge) would cause trench indentation.	Middle America Trench (SE Costa Rica) – Plio-Pleistocene to Present	- Subduction of an aseismic ridge (Cocos Ridge) causes an intense mechanical interactions and stress concentrations with the overriding plate being scraped and eroded, thinning the forearc crust and leading to a loss of forearc material. Although the removed material can accumulate ahead of the leading edge of the subducting relief reproducing underthrusting with a potential expression of shortening similar to a fold-and-thrust belt, this process is fundamentally different from a simple sliding mechanism, which would not result in the same level of material removal or structural alteration of the forearc.
Gravitational collapse and surficial erosion. Surficial erosion could remove large amount of sediment from the forearc resulting in its thinning.	Middle America Trench (SE Costa Rica) – Plio-Pleistocene to Present	- Surficial erosion does not explain large-scale forearc thinning – and also contradicts observations of continuous and undeformed forearc sedimentary sequences. Furthermore, if erosion removes large amounts of sediment from the forearc, then it can reduce loading and potentially lead to uplift rather than subsidence.

be accompanied by forearc shortening. Some authors imply that thickening at depth would cause subsidence of the forearc driven by flexural loading. However crustal thickening generates isostatic uplift: this is a well-known principle of mountain building and it has been reproduced in many analogue and numerical models. Even the role of subducting topography has been challenged to the point that in SE Costa Rica the subducting Cocos Ridge has been considered of less impact in shaping the margin than subducting seamounts. This conclusion is unrealistic not only given the magnitude of bathymetric relief and of crustal thickness, and broader and longer extent of interaction of a subducting ridge with the forearc when compared to a seamount, but also for the supporting geological evidence described in this paper.

Seismic interpretations of unconformities as marking a single time/depth subaerial event appear to be particularly problematic. For example, it is now increasingly accepted that the wide unconformities that form on rift shoulders are time-transgressive features (Péron-Pinvidic et al., 2007). While seismic imaging clearly provides key insights into the internal structure and evolution of forearcs, drill-core-based stratigraphic and dating constraints remain significantly less ambiguous than seismic-image-derived inferences. In general, drill-core-based constraints and isostatic considerations should be given higher observational weight than inferences based on seismic imaging alone.

We saw above that the 1980s drill-based inference of subduction erosion offshore the Northern Japan Trench remains strongly supported by critical drill-core-based observations that are inconsistent with forearc thinning due to wide regional stretching. The implied 'missing mass' is simply a discrepancy too large to be plausibly ignored. The subduction of the Cocos Ridge Plateau offshore Costa Rica has also been recently proposed to have led to strong horizontal compression and shortening that were associated with rapid forearc subsidence. Shortening, moreover, seems to be a highly implausible mechanism to generate large-scale subsidence, starting with its isostatic effects. Here too, the observed preservation of recent shallow portions of the forearc implies that the base of the outer forearc was removed during parts of its subduction history, even as its inboard inner forearc may have experienced local shortening and shortening-related uplift.

We appear to still be left with dueling processes that govern the evolution of subduction forearcs, the tectonic mode of forearc accretion that was first noted in the preserved rock record at the beginning of the Plate Tectonics revolution (Dickinson and Seely, 1979), and the subduction erosion mode that was seen in drill-core-based constraints on the tectonic subsidence and removal of many modern forearcs (Clift and Vannucchi, 2004). Alternation between accretion and subduction erosion has strongly shaped the evolution of Earth's continental crust. Even now many key details of the factors that control these oppositional processes – and their rates – still remain to be discovered and need to be tackled in an interdisciplinary manner.

Declaration of competing interest

Paola Vannucchi reports was provided by University of Florence. If there are other authors, they declare that they have no known competing financial interests or personal relationships that could have appeared to influence the work reported in this paper.

Data availability

All used data are public

Acknowledgments

We thank the editor Kelin Wang and two anonymous reviewers for the constructive comments that helped improving the manuscript.

References

Argus, D.F., Gordon, R.G., DeMets, C., 2011. Geologically current motion of 56 plates relative to the no-net-rotation reference frame. Geochem. Geophys. Geosyst. 12 (11).
Arroyo, I.G., Grevemeyer, I., Ranero, C.R., von Huene, R., 2014. Interplate seismicity at the CRISP drilling site: the 2002 Mw 6.4 Osa Earthquake at the southeastern end of the Middle America Trench. Geochem. Geophys. Geosyst. 15 (7), 3035–3050.
Arthur, M.A., Adelseck, C.G., 1980. Acknowledgements, introduction, and explanatory notes: The Japan Trench transect, Legs 56 and 57, Deep Sea Drilling Project. In: Party, Scientific (Ed.), Initial Reports of the Deep Sea Drilling Project, Volume 56–57: Washington. U.S. Got. printing Office, pp. 3–22.
Arthur, M.A., von Huene, R., Adelseck, C.G., 1980. Sedimentary evolution of the Japan fore-arc region off northern Honshu, Legs 56 and 57, Deep Sea Drilling Project. In: Scientific Party (Ed.), Initial Reports of the Deep Sea Drilling Project, Legs 56 and 57 (Part 1). U.S. Gov. Print. Off, Washington, D. C, pp. 521–612.
Aubouin, J., von Huene, R., et al., 1982. Initial Reports of the Deep Sea Drilling Program (Volume 67), Washington, DC. U.S. Govt. Printing Office.
Bangs, N.L., Cande, S.C., 1997. Episodic development of a convergent margin inferred from structures and processes along the southern Chile margin. Tectonics 16 (3), 489–503.
Bangs, N.L.B., Gulick, S.P.S., Shipley, T.H., 2006. Seamount subduction erosion in the Nankai Trough and its potential impact on the seismogenic zone. Geology 34 (8), 701–704.
Bangs, N.L., McIntosh, K.D., Silver, E.A., Kluesner, J.W., Ranero, C.R., 2015. Fluid accumulation along the Costa Rica subduction thrust and development of the seismogenic zone. J. Geophys. Res. Solid Earth 120 (1), 67–86.
Bangs, N.L., McIntosh, K.D., Silver, E.A., Kluesner, J.W., Ranero, C.R., 2016. A recent phase of accretion along the southern Costa Rican subduction zone. Earth Planet. Sci. Lett. 443, 204–215.
Bilek, S.L., Lay, T., 2018. Subduction zone megathrust earthquakes. Geosphere 14 (4), 1468–1500.
Bilek, S.L., Schwartz, S.Y., DeShon, H.R., 2003. Control of seafloor roughness on earthquake rupture behavior. Geology 31 (5), 455–458.
Bird, P., 2003. An updated digital model of plate boundaries. Geochem. Geophys. Geosyst. v. 4, no. 3.
Boston, B., Moore, G.F., Nakamura, Y., Kodaira, S., 2017. Forearc slope deformation above the Japan Trench megathrust: Implications for subduction erosion. Earth Planet. Sci. Lett. 462, 26–34.
Clift, P.D., MacLeod, C.J., 1999. Slow rates of subduction erosion estimated from subsidence and tilting of the Tonga forearc. Geology 27 (5), 411–414.
Clift, P., Vannucchi, P., 2004. Controls on tectonic accretion versus erosion in subduction zones: Implications for the origin and recycling of the continental crust. Rev. Geophys. 42 (2), RG2001. https://doi.org/10.1029/2003RG000127.
Clift, P.D., Pecher, I., Kukowski, N., Hampel, A., 2003. Tectonic erosion of the Peruvian forearc, Lima Basin, by subduction and Nazca Ridge collision. Tectonics 22 (3) p. art. no.-1023.
Davis, D.M., Suppe, J., Dahlen, A., 1983. Mechanics of fold-and-thrust belts and accretionary wedges. J. Geophys. Res. 88, 1153–1172.
DeMets, C., 2001. A new estimate for present-day Cocos-Caribbean plate motion: Implications for slip along the central American volcanic arc. Geophys. Res. Lett. 28 (21), 4043–4046.
DeMets, C., Gordon, R.G., Argus, D.F., Stein, S., 1990. Current plate motions. Geophys. J. Int. 101 (2), 425–478.
DeMets, C., Gordon, R.G., Argus, D.F., 2010. Geologically current plate motions. Geophys. J. Int. 181 (1), 1–80.
Dickinson, W.R., Seely, D.R., 1979. Structure and Stratigraphy of Forearc Regions. AAPG Bull. 63, 2–31.
Ding, M., Lin, J., 2016. Deformation and faulting of subduction overriding plate caused by a subducted seamount. Geophys. Res. Lett. 43 (17), 8936–8944.
Dominguez, S., Lallemand, S.E., Malavieille, J., von Huene, R., 1998. Upper plate deformation associated with seamount subduction. Tectonophysics 293 (3–4), 207–224.
Dominguez, S., Malavieille, J., Lallemand, S.E., 2000. Deformation of accretionary wedges in response to seamount subduction: Insights from sandbox experiments. Tectonics 19 (1), 182–196.
Edwards, J.H., Kluesner, J.W., Silver, E.A., Bangs, N.L., 2018. Pleistocene vertical motions of the Costa Rican outer forearc from subducting topography and a migrating fracture zone triple junction. Geosphere 14 (2), 510–534.
Edwards, J., Kluesner, J., Silver, E., Lauer, R., Bangs, N., Boston, B., 2021. In-situ mass balance estimates offshore Costa Rica. Geochem. Geophys. Geosyst. v, 22.
Fisher, D.M., Gardner, T.W., Marshall, J.S., Sak, P.B., Protti, M., 1998. Effect of subducting sea-floor roughness on fore-arc kinematics Pacific coast. Costa Rica: Geology 26 (5), 467–470.
Fisher, D.M., Gardner, T.W., Sak, P.B., Sanchez, J.D., Murphy, K., Vannucchi, P., 2004. Active thrusting in the inner forearc of an erosive convergent margin, Pacific coast, Costa Rica. Tectonics 23 (2) p. art. no.-TC2007.
Fujie, G., Kodaira, S., Kaiho, Y., Yamamoto, Y., Takahashi, T., Miura, S., Yamada, T., 2018. Controlling factor of incoming plate hydration at the North-Western Pacific margin: Nature. Communications v, 9.
Gardner, T., et al., 2001. Holocene forearc block rotation in response to seamount subduction, southeastern Peninsula de Nicoya. Costa Rica: Geology 29 (2), 151–154.
Hamahashi, M., Screaton, E., Tanikawa, W., Hashimoto, Y., Martin, K., Saito, S., Kimura, G., 2017. Normal faulting and mass movement during ridge subduction inferred from porosity transition and zeolitization in the Costa Rica subduction zone. Geochem. Geophys. Geosyst. 18 (7), 2601–2616.
Harris, R.N., Sakaguchi, A., Petronotis, K., the Expedition 344 Scientists, 2013. Proceeding IODP, Volume 344. Integrated Ocean Drilling Program, College Station, TX.
Hayes, G.P., Moore, G.L., Portner, D.E., Hearne, M., Flamme, H., Furtney, M., Smoczyk, G.M., 2018. Slab2, a comprehensive subduction zone geometry model. Science 362 (6410), 58–61.
Hayman, N.W., et al., 2012. Structural evolution of an inner accretionary wedge and forearc basin initiation, Nankai margin, Japan. Earth Planet. Sci. Lett. 353-354, 163–172.
Hilde, T.W.C., 1983. Sediment subduction versus accretion around the Pacific. Tectonophysics 99, 381–397.
Hoernle, K., van den Bogaard, P., Werner, R., Lissinna, B., Hauff, F., Alvarado, G., Garbe-Schonberg, D., 2002. Missing history (16-71 Ma) of the Galapagos hotspot: Implications for the tectonic and biological evolution of the Americas. Geology 30 (9), 795–798.
Husen, S., Kissling, E., Quintero, R., 2002. Tomographic evidence for a subducted seamount beneath the Gulf of Nicoya, Costa Rica: the cause of the 1990 Mw=7.0 Gulf of Nicoya earthquake. Geophys. Res. Lett. 29 (8) p. art. no.-1238.
Ingle, J., 1992. Subsidence of the Japan Sea: Stratigraphic evidence from ODP sites and onshore sections. Proc. Ocean Drill. Program Sci. Results 127 (128), 1197–1218.
Isacks, B., Oliver, J., Sykes, L.R., 1968. Seismology and the New Global Tectonics. J. Geophys. Res. 73 (18), 45.
Iwasaki, T., Levin, V., Nikulin, A., Iidaka, T., 2013. Constraints on the Moho in Japan and Kamchatka. Tectonophysics 609, 184–201.
Kagami, H., Karig, D.E., Coulbourn, W.Z., et al., 1986. Initial Reports of the Deep Sea Drilling Project (Volume 87). D.C., U.S., Government Printing Office, Washington, 985 p.
Karig, D.E., Sharman, G.F., 1975. Subduction and accretion at trenches. Geol. Soc. Am. Bull. 86, 13.
Karig, D.E., Kagami, H., DSDP Leg 87 Scientific Party, 1983. Varied responses to subduction in Nankai Trough and Japan Trench forearcs. Nature 304 (5922), 148–151.

Keller, G., 1980. Benthic foraminifers and paleobathymetry of the Japan Trench area, Leg 57, Deep Sea Drilling Project. In: Scientific Party (Ed.), Initial Reports of the Deep Sea Drilling Project, Legs 56 and 57 (Part 1). U.S. Gov. Print. Off., Washington, D. C, pp. 834–865.
Kimura, G., Silver, E.A., Blum, P., 1997. Proceedings of the Ocean Drilling Program, Initial Report, 170. College Station (TX), Ocean Drilling Program, 458 p.:
Kluesner, J.W., et al., 2013. High density of structurally controlled, shallow to deep water fluid seep indicators imaged offshore Costa Rica. Geochem. Geophys. Geosyst. 14 (3), 519–539.
Knipe, R.J., 1985. Footwall geometry and the rheology of thrust sheets. J. Struct. Geol. 7 (1), 1–10.
Kobayashi, D., LaFemina, P., Geirsson, H., Chichaco, E., Abrego, A.A., Mora, H., Camacho, E., 2014. Kinematics of the western Caribbean: Collision of the Cocos Ridge and upper plate deformation. Geochem. Geophys. Geosyst. 15 (5), 1671–1683.
Kolandaivelu, K.P., Harris, R.N., Lowell, R.P., Alhamad, A., Gregory, E.P.M., Hobbs, R. W., 2017. Analysis of a conductive heat flow profile in the Ecuador Fracture Zone. Earth Planet. Sci. Lett. 467, 120–127.
Kopp, H., 2013. Invited review paper: the control of subduction zone structural complexity and geometry on margin segmentation and seismicity. Tectonophysics 589, 1–16.
Lallemand, S.E., Schnurle, P., Manoussis, S., 1992. Reconstruction of Subduction Zone Paleogeometries and Quantification of Upper Plate Material losses Caused by Tectonic Erosion. J. Geophys. Res. Solid Earth 97 (B1), 217–239.
Lallemand, S., Peyret, M., Arcay, D., Heuret, A., 2024. Accretion versus erosion and sediment transfer balance near the subduction interface. Comptes Rendus. Géosci. 356 (S2), 27–51.
Lucke, O.H., Arroyo, I.G., 2015. Density structure and geometry of the Costa Rican subduction zone from 3-D gravity modeling and local earthquake data. Solid Earth 6 (4), 1169–1183.
Lundberg, N., Moore, J.C., 1981. Structural features of the Middle America Trench Slope off Southern Mexico, Deep Sea Drilling Project Leg 66. In: Watkins, J.S., Moore, J.C. (Eds.), Initial Reports of the Deep Sea Drilling Project LXVI. U.S. Govt. Printing Office, Washington, pp. 793–814.
MacMillan, I., Gans, P.B., Alvarado, G., 2004. Middle Miocene to present plate tectonic history of the southern central American Volcanic Arc. Tectonophysics 392 (1–4), 325–348.
Martinez-Loriente, S., Sallares, V., Ranero, C.R., Ruh, J.B., Barckhausen, U., Grevemeyer, I., Bangs, N., 2019. Influence of incoming plate relief on overriding plate deformation and earthquake nucleation: Cocos Ridge subduction (Costa Rica). Tectonics 38 (12), 4360–4377.
Martinod, J., Guillaume, B., Espurt, N., Faccenna, C., Funiciello, F., Regard, V., 2013. Effect of aseismic ridge subduction on slab geometry and overriding plate deformation: Insights from analogue modeling. Tectonophysics 588, 39–55.
McIntosh, K., Silver, E., Shipley, T., 1993. Evidence and mechanisms for fore-arc extension at the accretionary Costa Rica convergent margin. Tectonics 12 (6), 1380–1392.
Morell, K.D., 2015. Late Miocene to recent plate tectonic history of the southern Central America convergent margin. Geochem. Geophys. Geosyst. 16 (10), 3362–3382.
Morell, K.D., 2016. Seamount, ridge, and transform subduction in southern Central America. Tectonics 35 (2), 357–385.
Morell, K.D., Fisher, D.M., Gardner, T.W., La Femina, P., Davidson, D., Teletzke, A., 2011. Quaternary outer fore-arc deformation and uplift inboard of the Panama Triple Junction, Burica Peninsula. J. Geophys. Res. Solid Earth 116.
Morell, K.D., Fisher, D.M., Bangs, N., 2019. Plio-Quaternary outer forearc deformation and mass balance of the southern Costa Rica convergent margin. J. Geophys. Res. 124 (9), 9795–9815.
Morgan, J.K., Bangs, N.L., 2017. Recognizing seamount-forearc collisions at accretionary margins: Insights from discrete numerical simulations. Geology 45 (7), 635–638.
Morgan, J.P., Ranero, C.R., 2023. Chapter 21 - Roles of Serpentinization in Plate Tectonics and the Evolution of Earth's Mantle. In: Duarte, J.C. (Ed.), Dynamics of Plate Tectonics and Mantle Convection. Elsevier, pp. 511–537.
Morris, J.D., Villinger, H.W., Klaus, A., 2003. Proceedings of the Ocean Drilling Program, Initial Report, 205, College Station, Ocean Drilling Program, 75 (CD-ROM) p.:
Nasu, N., von Huene, R., Ishiwada, Y., Langseth, M., Brons, T., Honza, E., 1980. Interpretation of multichannel seismic reflection data, Legs 56 and 57, Japan Trench transect. Deep Sea Drilling Project. In: Party, S. (Ed.), Initial Reports of the Deep Sea Drilling Project (Volume 56–57). Government Printing Office, Washington, D.C., U. S, pp. 489–504.
Obana, K., et al., 2012. Normal-faulting earthquakes beneath the outer slope of the Japan Trench after the 2011 Tohoku earthquake: Implications for the stress regime in the incoming Pacific plate. Geophys. Res. Lett. 39.
Olsen, K.M., Bangs, N.L., Tréhu, A.M., Han, S., Arnulf, A., Contreras-Reyes, E., 2020. Thick, strong sediment subduction along south-Central Chile and its role in great earthquakes. Earth Planet. Sci. Lett. 538, 116195.
Park, J.-O., et al., 2021. Seismic Reflection Images of possible Mantle-Fluid conduits and Basal Erosion in the 2011 Tohoku Earthquake Rupture Area. Front. Earth Sci. v, 9.
Péron-Pinvidic, G., Manatschal, G., Minshull, T.A., Sawyer, D.S., 2007. Tectonosedimentary evolution of the deep Iberia-Newfoundland margins: evidence for a complex breakup history. Tectonics 26 (2).
Plank, T., Manning, C.E., 2019. Subducting carbon. Nature 574 (7778), 343–352.
Ranero, C.R., Morgan, J.P., McIntosh, K., Reichert, C., 2003. Bending, faulting, and mantle serpentinization at the Middle America Trench. nature 425, 367–373.
Ranero, C.R., Villasenor, A., Morgan, J.P., Weinrebe, W., 2005. Relationship between bend-faulting at trenches and intermediate-depth seismicity. Geochem. Geophys. Geosyst. 6.
Ranero, C.R., et al., 2008. The hydrogeological system of erosional convergent margins and its influence on tectonics and interplate seismogenesis. Geochem. Geophys. Geosyst. 9, Q03. https://doi.org/10.1029/2007GC001679.
Regalla, C., Fisher, D.M., Kirby, E., Furlong, K.P., 2013. Relationship between outer forearc subsidence and plate boundary kinematics along the Northeast Japan convergent margin. Geochem. Geophys. Geosyst. 14 (12), 5227–5243.
Ruh, J.B., Sallarès, V., Ranero, C.R., Gerya, T., 2016. Crustal deformation dynamics and stress evolution during seamount subduction: High-resolution 3-D numerical modeling. J. Geophys. Res. Solid Earth 121 (9), 6880–6902.
Rupke, L.H., Morgan, J.P., Hort, M., Connolly, J.A.D., 2004. Serpentine and the subduction zone water cycle. Earth Planet. Sci. Lett. 223 (1–2), 17–34.
Ryan, W.B.F., Carbotte, S.M., Coplan, J., O'Hara, S., Melkonian, A., Arko, R., Weissel, R. A., Ferrini, V., Goodwillie, A., Nitsche, F., Bonczkowski, J., Zemsky, R., 2009. Global Multi-Resolution Topography (GMRT) synthesis data set. Geochem. Geophys. Geosyst. 10, Q03014. https://doi.org/10.1029/2008GC002332.
Saffer, D.M., Tobin, H.J., 2011. Hydrogeology and Mechanics of Subduction Zone Forearcs: Fluid Flow and Pore pressure. In: Jeanloz, R., Freeman, K.H. (Eds.), Annual Review of Earth and Planetary Sciences, vol. 39, pp. 157–186.
Sak, P.B., Fisher, D.M., Gardner, T.W., 2004. Effects of subducting seafloor roughness on upper plate vertical tectonism: Osa Peninsula, Costa Rica. Tectonics 23, TC1017. https://doi.org/10.1029/2002TC001474.
Sallares, V., Charvis, P., Flueh, E.R., Bialas, J., 2003. Seismic structure of Cocos and Malpelo Volcanic Ridges and implications for hot spot-ridge interaction. J. Geophys. Res. Solid Earth 108 (B12).
Sato, H., 1994. The relationship between late Cenozoic tectonic events and stress-field and basin development in Northeast Japan. J. Geophys. Res. 99 (B11), 22261–22274.
Schindlbeck, J.C., Kutterolf, S., Freundt, A., Straub, S.M., Vannucchi, P., Alvarado, G.E., 2016. Late Cenozoic tephrostratigraphy offshore the southern Central American Volcanic Arc: 2. Implications for magma production rates and subduction erosion. Geochem. Geophys. Geosyst. 17 (11), 4585–4604.
Sitchler, J.C., Fisher, D.M., Gardner, T.W., Protti, M., 2007. Constraints on inner forearc deformation from balanced cross sections, Fila Costena thrust belt, Costa Rica. Tectonics 26 (6), TC6012.
Stern, C.R., 2011. Subduction erosion: rates, mechanisms, and its role in arc magmatism and the evolution of the continental crust and mantle. Gondwana Res. 20 (2–3), 284–308.
Straub, S.M., Gomez-Tuena, A., Vannucchi, P., 2020. Subduction erosion and arc volcanism. Nat. Rev. Earth Environ. 1 (11), 574–589.
Sun, T., Saffer, D., Ellis, S., 2020. Mechanical and hydrological effects of seamount subduction on megathrust stress and slip. Nat. Geosci. 13 (3), 249–255.
Takahashi, N., et al., 2004. Seismic structure and seismogenesis off Sanriku region, northeastern Japan. Geophys. J. Int. 159 (1), 129–145.
Tsuru, T., Park, J.O., Takahashi, N., Kodaira, S., Kido, Y., Kaneda, Y., Kono, Y., 2000. Tectonic features of the Japan Trench convergent margin off Sanriku, northeastern Japan, revealed by multichannel seismic reflection data. J. Geophys. Res. Solid Earth 105 (B7), 16403–16413.
Tsuru, T., Park, J.O., Miura, S., Kodaira, S., Kido, Y., Hayashi, T., 2002. Along-arc structural variation of the plate boundary at the Japan Trench margin: Implication of interplate coupling. J. Geophys. Res. Solid Earth 107 (B12).
Turcotte, D.L., McAdoo, D.C., Caldwell, J.G., 1978. An elastic-perfectly plastic analysis of the bending of the lithosphere at a trench. Tectonophysics 47 (3), 193–205.
van Rijsingen, E., Funiciello, F., Corbi, F., Lallemand, S., 2019. Rough Subducting Seafloor Reduces Interseismic Coupling and Mega-Earthquake Occurrence: Insights from Analogue Models. Geophys. Res. Lett. 46 (6), 3124–3132.
Vannucchi, P., Ranero, C.R., Galeotti, S., Straub, S.M., Scholl, D.W., McDougall-Ried, K., 2003a. Fast rates of subduction erosion along the Costa Rica Pacific margin: Implications for nonsteady rates of crustal recycling at subduction zones: Journal of Geophysical Research-Solid. Earth 108 (B11).
Vannucchi, P., Ranero, C.R., Galeotti, S., Straub, S.M., Scholl, D.W., McDougall-Ried, K., 2003b. Fast rates of subduction erosion along the Costa Rica Pacific margin: Implications for nonsteady rates of crustal recycling at subduction zones. J. Geophys. Res. 108 (B11), 2511. https://doi.org/10.1029/2002JB002207.
Vannucchi, P., Galeotti, S., Clift, P.D., Ranero, C., von Huene, R., 2004. Long Term Subduction Erosion along the Middle America Trench offshore Guatemala. Geology 32 (7), 617–620.
Vannucchi, P., Fisher, D.M., Gardner, T.W., Bier, S., 2006. From seamount accretion to tectonic erosion: Formation of Osa Mélange and the effects of Cocos Ridge subduction in southern Costa Rica. Tectonics 25 (TC2004).
Vannucchi, P., Ujiie, K., Stroncik, N., 2012. The Expedition 334 Scientists. In: Proceedings IODP. Integrated Ocean Drilling Program Management International, Inc., Tokyo.
Vannucchi, P., Sak, P.B., Morgan, J.P., Ohkushi, K., Ujiie, K., Scientists, I.E.S., 2013. Rapid pulses of uplift, subsidence, and subduction erosion offshore Central America: Implications for building the rock record of convergent margins. Geology 41, 995–998.
Vannucchi, P., Morgan, J.P., Balestrieri, M.L., 2016a. Subduction erosion, and the de-construction of continental crust: the Central America case and its global implications. Gondwana Res. 40, 184–198.
Vannucchi, P., Morgan, J.P., Silver, E.A., Kluesner, J.W., 2016b. Origin and dynamics of depositionary subduction margins. Geochem. Geophys. Geosyst. 17 (6), 1966–1974.
Vannucchi, P., Spagnuolo, E., Aretusini, S., Di Toro, G., Ujiie, K., Tsutsumi, A., Nielsen, S., 2017. Past seismic slip-to-the-trench recorded in Central America megathrust. Nat. Geosci. 10 (12), 935–940.
von Huene, R., Aubouin, J., et al., 1984. Initial Reports of the Deep Sea Drilling Project (Volume 84), Washington, DC. U.S. Govt, Printing Office.

von Huene, R., Culotta, R., 1989. Tectonic erosion at the front of the Japan Trench convergent margin. Tectonophysics 160, 75–90.
von Huene, R., Lallemand, S., 1990. Tectonic Erosion along the Japan and Peru Convergent margins. Geol. Soc. Am. Bull. 102 (6), 704–720.
von Huene, R., Scholl, D.W., 1991. Observations at Convergent margins concerning Sediment Subduction, Subduction Erosion, and the growth of Continental- Crust. Rev. Geophys. 29 (3), 279–316.
von Huene, R., et al., 1978. Japan Trench transected on Leg 57. Geotimes 23 (4), 16–21.
von Huene, R., Langseth, M., Noriyuki, N., Hakuyu, O., 1982. A summary of Cenozoic tectonic history along the IPOD Japan Trench transect. Geol. Soc. Am. Bull. 93, 829–846.
von Huene, R., Ranero, C.R., Weinrebe, W., Hinz, K., 2000. Quaternary convergent margin tectonics of Costa Rica, segmentation of the Cocos Plate, and central American volcanism. Tectonics 19 (2), 314–334.
von Huene, R., Ranero, C.R., Vannucchi, P., 2004. Generic model of subduction erosion. Geology 32 (10), 913–916.
Wang, K., Bilek, S.L., 2011. Do subducting seamounts generate or stop large earthquakes? Geology 39 (9), 819–822.
Wang, K., Hu, Y., 2006. Accretionary prisms in subduction earthquake cycles: the theory of dynamic Coulomb wedge. J. Geophys. Res. 111 (B6), B06410. https://doi.org/10.01029/02005JB004094.
Wang, Z., Zhao, D.P., 2005. Seismic imaging of the entire arc of Tohoku and Hokkaido in Japan using P-wave, S-wave and sP depth-phase data. Phys. Earth Planet. Inter. 152 (3), 144–162.
Wang, K., Hu, Y., von Huene, R., Kukowski, N., 2010. Interplate earthquakes as a driver of shallow subduction erosion. Geology 38 (5), 431–434.
Watkins, J.S., Moore, J.C., et al., 1981. Initial Reports of the Deep Sea Drilling Project (Volume 66), Washington, DC, US. U.S. Govt, Printing Office.
Whittaker, J.M., Goncharov, A., Williams, S.E., Müller, R.D., Leitchenkov, G., 2013. Global sediment thickness data set updated for the Australian-Antarctic Southern Ocean. Geochem. Geophys. Geosyst. 14 (8), 3297–3305.
Xu, S.H., Zhao, X.X., Li, Y.X., Liu, X.Y., Chen, W.W., 2021. Pulsed vertical displacement and subsequent shearing in the forearc of the Costa Rican convergent margin: evidence from paleomagnetic results of IODP site U1413. Mar. Geol. 441.
Zeumann, S., Hampel, A., 2015. Deformation of erosive and accretive forearcs during subduction of migrating and non-migrating aseismic ridges: results from 3-D finite element models and application to the central American, Peruvian, and Ryukyu margins. Tectonics 34 (9), 1769–1791.
Zeumann, S., Hampel, A., 2016. Three-dimensional finite-element models on the deformation of forearcs caused by aseismic ridge subduction: the role of ridge shape, friction coefficient of the plate interface and mechanical properties of the forearc. Tectonophysics 684, 76–91.